A Micrometer-sized *Isothermal* Stirling Engine Operating Between Engineered Reservoirs

A Thesis

Submitted in partial fulfilment for the degree of

MASTER OF SCIENCE

as a part of Integrated Ph.D. programme

(Materials Science)

by

NILOYENDU ROY

CHEMISTRY AND PHYSICS OF MATERIALS UNIT

JAWAHARLAL NEHRU CENTRE

FOR ADVANCED SCIENTIFIC RESEARCH

(A Deemed University)

Bangalore - 560064

APRIL 2018

To Prof. Richard Feynman who planted all these ideas

Declaration

I hereby declare that the matter embodied in the thesis entitled **"A Micrometer-sized *Isothermal* Stirling Engine Operating Between Engineered Reservoirs"** is the result of investigations carried out by me at the Chemistry and Physics of Materials Unit, Jawaharlal Nehru Centre for Advanced Scientific Research, Bangalore, India, under the supervision of Prof. Rajesh Ganapathy and that it has not been submitted elsewhere for the award of any degree or diploma.

In keeping with the general practice in reporting scientific observations, due acknowledgement had been made whenever the work described is based on the findings of other investigators.

Niloyendu Roy

Certificate

I hereby certify that the matter embodied in this thesis entitled **"A Micrometer-sized *Isothermal* Stirling Engine Operating Between Engineered Reservoirs"** has been carried out by Mr. Niloyendu Roy at the Chemistry and Physics of Materials Unit, Bangalore, India, under my supervision and that it has not been submitted elsewhere for the award of any degree or diploma.

Prof. Rajesh Ganapathy

Acknowledgements

I am grateful to my research superviser Prof. Rajesh Ganapathy for all the inspirations and for providing me the best guidance I could ever think of during the research.

I sincerely thank Prof. Ajay Sood for all the inspirations and the enlightening discussion which helped me a lot during the research.

I sincerely thank Prof. Udo Seifert for the enlightening discussion about the research project.

I thank Mr. Sudeesh Krishnamurthy for the useful discussions and for providing me the polystyrene particles with diameter of 5 micrometer which were used during all the experiments.

I am extremely thankful to Mr. Nathan Leroux who worked with me for three moths in the past year. He contributed sufficiently during our collaboration with him.

I am grateful to my lab mates Mrs. Divya G, Ms. Srimayee Mukherjee, Mr. Manodeep Mondal, Mr. Navneet Mondal, Ms Pragya Arora and past member of the lab Dr. Chandan Mishra for their constant support and for crating an awesome lab environment. I am also grateful to my batch mates in JNCASR for their constant support.

I am thankful to Prof. C.N.R. Rao for being a constant source of inspiration and for providing one of the most advanced research facilities in the Sheikh Saqar Laboratories

in JNCASR.

I am thankful to CPMU chairman Prof. Chandrabhas Narayana for the support and for valuable anduseful advices. I also thank Int. PhD co-ordinators for their valuable advices. I thank all the instructors of the courses I have taken in JNCASR for their valuable lessons.

I am grateful to Prof. Rajshekhar Bhattacharyya for the great teaching and enlightening discussions and for inspiring me to pursue research in physics during my undergraduate days.

I am grateful to all my dear friends for giving me constant support and making my life wonderful. I am also grateful to my most special friend who always supported me and made my life beautiful.

I am grateful to my parents for awesome childhood I spent and for inspiring me for research. I am also grateful to my brother who always a constant faith and supported me all the time. I will always be grateful to my grand parents for all their lessons which always helped me.

Preface

In this thesis, we present a novel experimental technique to engineer thermal and active reservoirs and show how micrometer-sized heat engines can be operated between such reservoirs.

This thesis consists of three chapters. Chapter 1 provides the basic framework of stochastic thermodynamics essential to describe the operation of micro-mechanical machines and introduces all micrometer-sized stochastic heat engines which has been realised in experiments so far. Chapter 2 describes the experimental setup we developed and the procedure we followed for reservoir engineering. This chapter also describe the procedure involved in making an isothermal heat engine operating between such engineered reservoirs. In Chapter 3, I discuss in detail the methods to quantify the properties of such heat engines and interpret some important thermodynamic aspects of it from our experimental results.

Contents

List of Figures

Chapter 1

Introduction

Miniaturization is a key driver of present day science and technology. Apart from electronic devices and memory chips, machines with movable parts are also at the frontier of miniaturization. Some of the most exotic applications of such tiny mechanical machines could be from collective robotics to micron-sized robot surgeons inside human bodies. At small enough length scales, the physical construction and the properties of such small machines are different from their macroscopic counterparts. Although the concept of miniaturization of mechanical machines was first introduced by Prof. Richard Feynman during his lecture called "Tiny Machines" in 1984 [27, 26], only recently it has been made possible to experimentally realise some simple mechanical machines at very small length scales such as a single colloid or even a single atom [2, 29, 21, 18, 4, 14, 28, 17].

Heat engines which convert heat into mechanical energy has played a pivotal role in human civilization since the time of industrial revolution. Sadi Carnot developed a thermodynamic basis for how such heat engines work. Heat engines are machines which in one cycle of operation, take a certain amount of heat Q_H from a hot reservoir, performs a mechanical work W on the virtue of the heat taken and give away a certain amount of heat Q_C to a cold reservoir (Figure 1.1 (a)). Efficiency η of such engines is given by the

ratio of work done to the heat taken from the hot reservoir. i.e.

$$\eta = W/Q_H \tag{1.1}$$

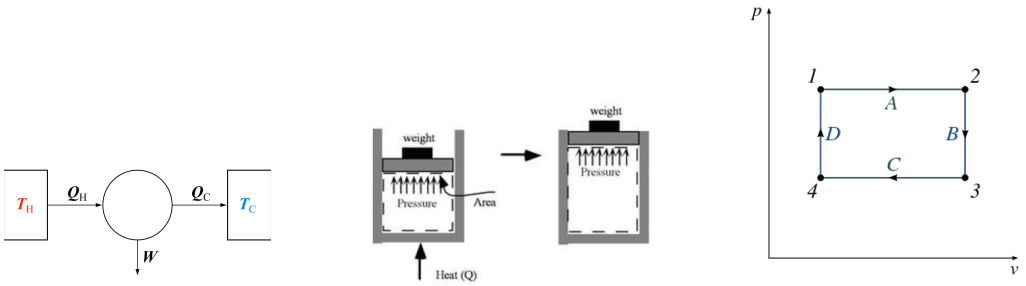

(a) (b) (c)

Figure 1.1: (a): Schematic for one cycle of operation of the heat engine where the hot reservoir is at temperature T_H and the cold bath is at temperature T_C, (b): real construction of a heat engine, (c): cycle of operation is shown in a $\mathcal{P} - v$ diagram. Images in this figure has been adopted from Google Images.

The first and second law of thermodynamics set a constraint to this quantities. The first law of thermodynamics which is the law of conservation of energy says the heat taken from the hot reservoir dQ at any instant is equal to the sum of work done $đW$ and increase in the internal energy dU of the engine. Heat engines consists of a cylinder filled with a gas and a piston sliding across the cylinder (Figure 1.1 (b)). If heat is absorbed by the gas inside through the walls of the cylinder in contact with the hot reservoir, internal energy of the gas increases which leads to an increase of pressure on the piston. So the piston moves up and finally achieve an equilibrium state in which the pressure $\mathcal{P}$ equalises the weight. The work done by the engine is given by the pressure $\mathcal{P}$ times the increase in volume dV of the system i.e. $đW = \mathcal{P}dv$. So the first law can be written as

$$đQ = dU + đW = dU + \mathcal{P}dv \tag{1.2}$$

The exposure to hot and cold reservoir happens periodically due to the cyclic operation of the engine and as a result the system traces a cyclic path (Figure 1.1 (c)) in the $\mathcal{P} - v$

diagram. The area under the loop in the $\mathcal{P} - v$ diagram is therefore the work done of the engine in one cycle.

Now the second law of thermodynamics sets a maximum limit to the efficiency of a Carnot engine. If the changes in the system are made infinitely slow i.e. quasistatically, irrespective of the specific protocol for the operation the efficiency of the engine is the same and it is only dependent upon the temperature of the hot and cold reservoir.

$$\eta = W/Q_H = 1 - T_C/T_H \tag{1.3}$$

In this thesis we will be discussing about heat engines which consists of only one colloidal particle suspended in a liquid in place of the gas inside the cylinder which has of the order of 10^{24} atoms. When the system consists of one colloidal particle having size of the order of micrometers, the system size is decreased by six orders of magnitude compared to classical macroscopic systems. At these length scales, the statistical fluctuation in the physical quantities of the system becomes important and thermodynamics has to be reformulated in terms of a single fluctuating trajectory like the Brownian trajectory of a colloidal particle in a suspension.

1.1 Stochastic Thermodynamics

It was first realised by Sekimoto [34, 35], that the two central concepts of classical thermodynamics such as work done and heat exchanged can be meaningfully assigned to a single fluctuating trajectory of a colloidal particle performing Brownian motion in a fluid. These fluctuating quantities entering the first law gives rise to something called stochastic energetics as coined by him. Stochastic thermodynamics describes the transformations of the small systems like colloidal particles,enzymes and molecular motors, bio-polymers

like DNA,RNA etc.

One of the simplest ways to formulate stochastic thermodynamics is to consider a colloidal particle suspended in a fluid and held in a potential. Let us consider that the potential V which is a function of the spatial variable x can be manipulated with respect to time using a control parameter λ. Now the overdamped motion of the colloidal particle with trajectory $x(\tau)$ in a potential $V(x,\lambda)$ can be described using three equivalent descriptions, namely the Langevin equation, the path integral and the Fokker-Plank equation [33, 32].

Langevin equation for such a colloidal particle is as follows:

$$\dot{x} = \mu F(x,\lambda) + \zeta = \mu(-\partial_x V(x,\lambda) + f(x,\lambda)) + \zeta \tag{1.4}$$

Here, the systematic force on the particle $F(x,\lambda)$ can have two contributions, one due to the conservative potential $V(x,\lambda)$ and the other can be a force $f(x,\lambda)$ acting directly on the particle. In addition to the systematic force, the colloidal particle is being bombarded by the liquid molecules giving rise to a noisy force on the particle which appears as the noise term ζ in the Langevin equation. If the dynamics is being observed at a much larger time scale compared to the time of collision between the colloidal particle and the solvent molecules, the correlation in ζ is as follows:

$$\langle \zeta(\tau)\zeta(\tau')\rangle = 2D\delta(\tau - \tau') \tag{1.5}$$

Where D is the diffusion constant. In equilibrium at temperature T, μ and D are related by the Einstein's relation

$$D = T\mu. \tag{1.6}$$

According to the Langevin equation any trajectory $x(\tau)$ of the colloidal particle starting

at $x(0) = x_0$ is possible with a probability

$$p[x(\tau)|x_0] = \mathcal{N} exp[-\mathcal{A}([x(\tau), \lambda(\tau)])] \tag{1.7}$$

where

$$\mathcal{A}([x(\tau), \lambda(\tau)]) = \int_0^t d\tau[(\dot{x} - \mu F)^2/4D + \mu \partial_x F/2] \tag{1.8}$$

is called the **action** associated with the trajectory. $\mathcal{N}$ is the normalisation factor and the last term in the right hand side of equation (1.8) is due to the Stratonivich convention [33].

With the help of above the expectation value of any path dependent observable $\Omega[x(\tau)]$ can now be theoretically calculated by doing a path integral with a weight $p[x(\tau)|x_0]$ as follows:

$$\langle \Omega[x(\tau)] \rangle = \int dx_0 \int \Omega[x(\tau)] p[x(\tau)|x_0] p_0(x_0) \; d[x(\tau)] \tag{1.9}$$

1.1.1 Stochastic energetics

The first thermodynamic interpretation of Langevin dynamics starts with the incorporation of first law to the particle's trajectory. Similar to classical thermodynamics , for a single particle the first law reads as the heat dissipated by the particle is equal to the sum of the change in internal energy of the particle and the work done on the particle.

$$đQ = dU + đW \tag{1.10}$$

The work done on the particle is due to the change in the potential and the force $f(x, \lambda(\tau))$ applied to the particle.

$$đW = -(\partial V/\partial \lambda) + f \, dx \tag{1.11}$$

thus the heat dissipated is given by

$$đQ = F \, dx \tag{1.12}$$

Integrating the above two equations over time t we find the expression for heat and work for the fluctuating trajectory to be

$$W[x(\tau)] = \int_0^t [(\partial V/\partial\lambda)\dot{\lambda} + f\dot{x}]\, d\tau \tag{1.13}$$

$$Q[x(\tau)] = \int_0^t \dot{q}\, dt = \int_0^t F\dot{x}\, d\tau \tag{1.14}$$

Therefore in principle these quantities can be theoretically calculated using equation (1.9).

Most interestingly, with these definitions of work and heat within the Langevin framework one can quantify the extent of irreversibility in terms of heat dissipated. Let us consider a trajectory $x(\tau)$ in the time interval $(0, t)$ and the time reversed trajectory $\tilde{x}(\tau)$ so that $\tilde{x}(\tau) = x(t-\tau)$ then the heat dissipated can be written as

$$Q[x(\tau)] = T\,\frac{\mathcal{A}([x(\tau),\lambda(\tau)])}{\mathcal{A}([x(t-\tau),\lambda(t-\tau)])} = T\,\ln\frac{p[x(\tau),\lambda(\tau)]}{p[\tilde{x}(\tau),\tilde{\lambda}(\tau)]} \tag{1.15}$$

One of the biggest advantages of stochastic thermodynamics over classical thermodynamics towards understanding non-equilibrium systems is that one can quantify the extent of irreversibility and get a measure of how far the system is from equilibrium. In chapter 3 we will discuss about some more quantities through which the extent of irreversibility can be measured and show how these quantities can be used to optimise micro heat engines to work in different modes of operation.

1.2 Stochastic Heat Engines

One of the most simple and elegant protocol for practically realizable microscopic heat engine was suggested by Udo Seifert [31]. The heat engine is made up of a single colloidal particle in a time dependent potential $V[x(\tau), \lambda(\tau)]$. The contraction and expansion of the engine is given in terms of increase or decrease of the stiffness of the potential because

at higher stiffness the width of the probability distribution function of particle's position from it's mean shrinks thus effectively the volume accessible to the particle decreases as show in Figure 1.1.

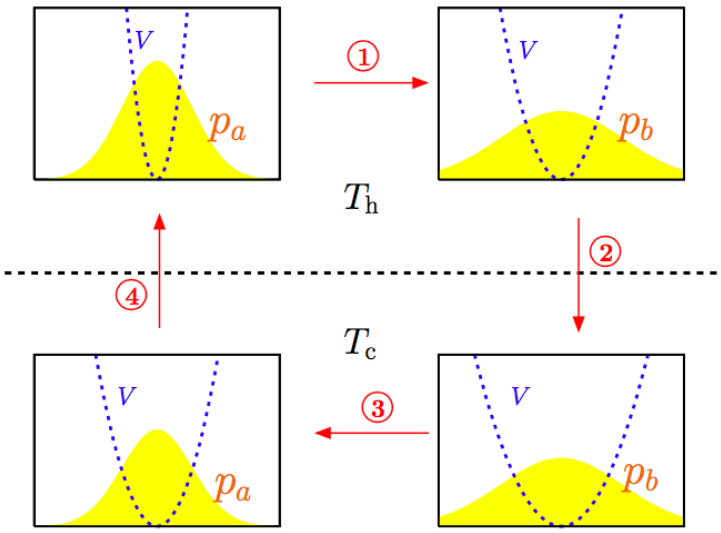

Figure 1.2: Schematic of the cycles of a stochastic heat engine operating between two reservoirs at temperatures T_h and T_c with $T_h > T_c$. The dotted curve represents the one dimensional potential $V(x,\tau)$ and the filled yellow curve represents the probability distribution function $p(x,\tau)$. This figure is adopted from [31]

Steps 1 and 3 in Figure 1.2 represents isothermal expansion and contraction respectively where the stiffness of the potential is changed keeping the temperature of the liquid constant. Steps 2 and 4 represents adiabatic expansion and compression respectively where the probability distribution function $p(x,\tau)$ is kept constant making this protocol of Carnot type. Although the extensive nature of the work done and efficiency of such a engine was studied, the experimental realization was not straight forward.

The first experimental realisation of such a stochastic heat engine was carried out by Bechinger and co-workers[2] where instead of a Carnot cycle, Stirling cycle has been performed.

1.2.1 Experimental Realisation of a Brownian Stirling Heat Engine

The Brownian Stirling engine was realised by optically trapping a melamine sphere(suspended in water) of diameter 2.94 μm by tightly focusing a laser beam on the particle [2]. Inside such an optical trap the colloidal bead experiences to a good approximation a parabolic potential V given by

$$V(R,k) = \frac{1}{2}kR^2 \tag{1.16}$$

where k is the stiffness of the potential and R is the distance of the particle from its mean position. Under such a potential the probability distribution function $p(x,t)$ of the particle is a Gaussian with its standard deviation being the measure of temperature. The Stirling engine protocol was realised in this system as following (Figure 1.3):

Step 1: Keeping the temperature of the water constant at $T_c = 22°C$ the trap stiffness was changed from $k_{min} = 281\, fN\mu m^{-1}$ to $k_{max} = 1180\, fN\mu m^{-1}$. This step corresponds to an isothermal compression which takes the system from state (1) to state (2) as shown in Figure 1.3 .

Step 2: Keeping the stiffness of the trap constant at k_{max} the water medium was heated almost instantaneously to the temperature $T_c = 86°C$ by laser heating. This step corresponds to an isochoric transition from temperature T_c to T_h.

Step 3: In this step an isothermal compression was performed by keeping the temperature constant at T_h and bringing down the stiffness from k_{max} to k_{min}.

Step 4: An isochoric transition was performed by switching off the heating laser at constant stiffness. Thus the system comes back to its initial state (1).

These steps are carried out in cycle and from the particle's trajectory the work done and efficiency was measured in real time. The time-dependent work is calculated by

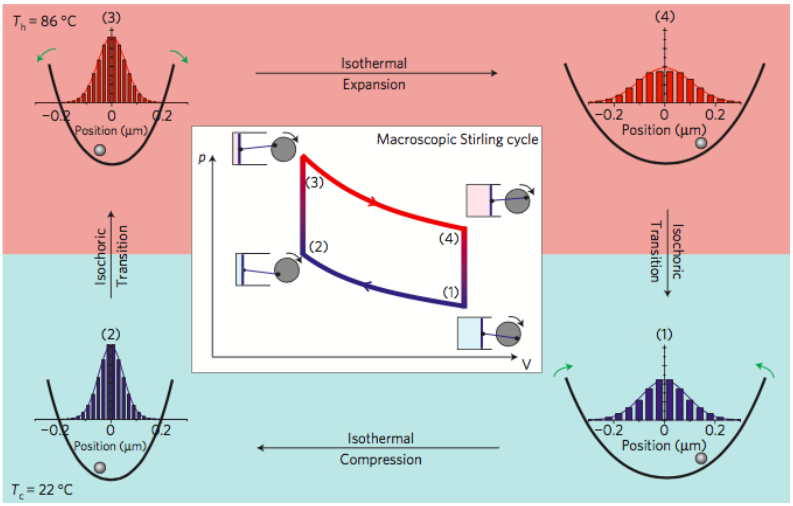

Figure 1.3: Schematic of the Stirling protocol. This figure is adopted from [2]

integration along the stochastic trajectory as follows:

$$W(t) = \int_0^t \frac{\partial V(R', t')}{\partial t'} \, dt' \tag{1.17}$$

As because there is no change in volume i.e. the stiffness k during the isochoric transitions it is clear that they don't contribute to the work done. If τ is the cycle duration which is twice the time it takes to go from state (1) to state (2) or from state (3) to state (4) then the work done per cycle W_n is given by

$$W_n = \int_{n\tau}^{(n+1)\tau} \frac{\partial V(R', t')}{\partial t'} \, dt' \tag{1.18}$$

For cycle duration $\tau = 12s$ and over about 100 cycles the engine extracts nearly $20k_BT$ of energy from its surrounding as shown by the black line in Figure 1.4 (a)

The fluctuation in the work done is clearly seen for this stochastic engine and the probability distribution of the work done also turns out to be Gaussian with negative and positive mean for the forward and reverse protocol respectively.

Apart from the average work done per cycle $\overline{W}$, power P and efficiency η of the engine was also studied as a function of cycle duration keeping the temperature difference

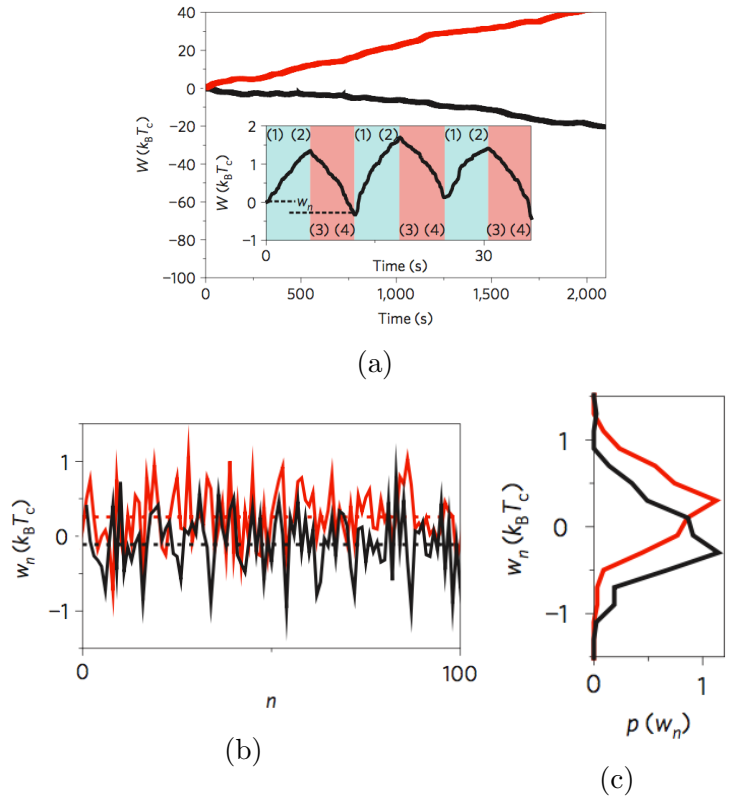

(a)

(b)

(c)

Figure 1.4: (a) The black line represents work done as a function of time for the protocol described above and the black line represents work done for the reverse protocol where the engine works as a heat pump which provides energy to the surroundings, (b) work done per cycle W_n with respect to the cycle number n, (c) the probability distribution of the work done per cycle. This figure is adopted from [2].

constant. The results are shown in Figure 1.5. It is seen that the work done (red line in Figure 1.5 (a)) asymptotically reaches its maximum at infinite cycle durations which is consistent to theoretical predictions from stochastic thermodynamics [2, 32] and also macroscopic thermodynamics. But for the cycle durations lower than $3.6s$, the engine starts stalling not being able to perform work thus the work done is positive(for the forward protocol) and the engine starts working as a heat pump. This can be explained in terms of irreversibility as follows. When the rate of change of stiffness is rapid, it is harder for the particle to equilibrate at each trap stiffness $k(t)$ and expand to the effective volume available to it. Because of the fact that work done is proportional to the displacement of the particle from the mean position, the poorer it spans the available volume, the lesser is the work done. And when the rate of change of trap stiffness is

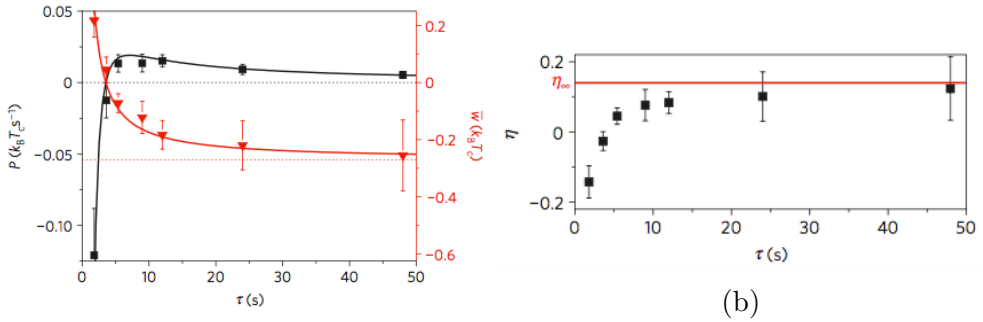

(a) (b)

Figure 1.5: (a) Dependence of power(black line) $p = \overline{W}/\tau$ as a function of cycle duration τ and dependence of work done(red line) per cycle $\overline{W}$ (b) dependence of efficiency η with respect to cycle duration τ. This figure is adopted from [2].

comparable to the equilibration time of the particle in the trap, it starts stalling. The average work done per cycle with respect to the cycle duration can be decomposed into two components.

$$\overline{W} = \overline{W}_{\infty} + \overline{W}_{diss} \tag{1.19}$$

Here $\overline{W}_{\infty}$ is the work done at infinite cycle duration which is theoretically given by(in two dimensions)

$$\overline{W}_{\infty} = 2k_B[T_c - T_h] \ln \sqrt{\frac{k_{max}}{k_{min}}} \tag{1.20}$$

and $\overline{W}_{diss}$ is the dissipative irreversible work which is due to the rapid change of the trap stiffness. The expression for $\overline{W}_{diss}$ at best can be theoretically written as

$$\overline{W}_{diss} = \frac{\Sigma}{\tau}. \tag{1.21}$$

Here the parameter Σ is a constant which depends upon the specific experimental parameters.

On the other hand the power with respect to cycle duration has a special feature. With decreasing cycle duration it increases then shows a peak at $\tau = 7s$ and finally crosses zero bellow 3.6s (exactly at the same τ at which work done crosses zero). The black line in Figure 1.5 (a) is the fit of the derivative of the right hand side of the equation (1.19).

This nature of the power of a heat engine was first predicted by Curzon and Ahlborn [9] for macroscopic heat engines.

Efficiency also asymptotically approaches the maximum at infinite cycle duration and decreases for smaller cycle duration as shown in Figure 1.5 (b). Most practically relevant efficiency is the one at maximum power called Curzon-Ahlborn efficiency η_{CA} is 0.075 for this engine.

1.2.2 Reservoir Engineering and the Brownian Carnot Engine

Unlike isochoric processes, an adiabatic process for a single particle is very hard to realise. Because it is impossible to isolate a colloidal particle adiabatically from the heat bath. This difficulity has been overcome by the method of reservoir engineering [22, 20, 5].

Reservoir Engineering

In addition to the noisy environment on the particle due to bombardment of liquid molecules surrounding it, it is possible to artificially apply noisy force on the particle and create an effective heat bath in which the properties of the particle's trajectory are different.

Fluctuating electric field for example has been used to additionally kick a charged colloidal particle [23, 22].
If one looks at the power spectral density of particle's vibration in an optical trap, it turns out to be Lorentzian. By applying noisy electric field across the particle with a suitable protocol for the electric field noise, one can maintain the Lorentzian nature of the power spectral density(PSD) of the particle's effective vibration in the trap, the artificial noise can be considered as white noise (Figure 1.6 (a)). Now in addition to this if it is possible to maintain the Gaussian nature of the particle's probability distribution then in the Langevin equation (1.4) for the effective dynamics of the particle the noise

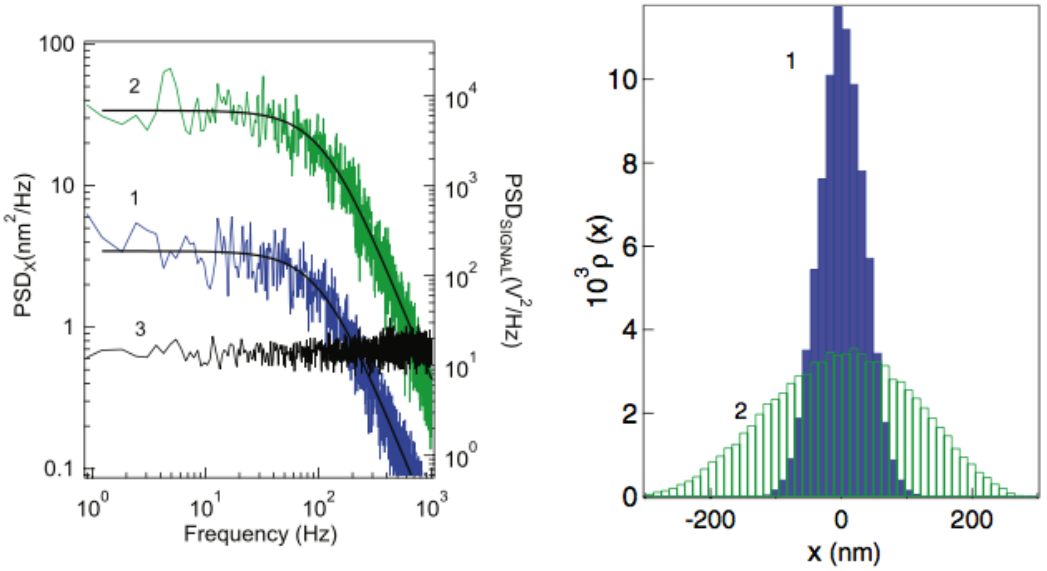

(a) (b)

Figure 1.6: (a)Black curve is the PSD of electric field noise, Blue curve is the PSD of particle's displacement in water at 300K without the presence of electric field noise, Green curve is the PSD of the particle's displacement with electric field noise on. (b) Blue histogram is the probability distribution function(pdf) of the particle in water at 300k and green histogram is the corresponding pdf with electric field noise on which corresponds to 3000k. This figure is adopted from [23].

term ζ is again a Gaussian white noise and an effective temperature of the particle can be defined in a similar way. It has been made experimentally possible by Dmitri Petrov and co-workers [23] thus the particle can be heated to several thousand kelvins (Figure 1.6 (a),(b)) by electric field noise without physically heating the medium. The effective temperature is measured from the information of the width of the probability distribution of the particle.

$$\frac{1}{2}k\langle x^2\rangle = \frac{1}{2}k_B T \tag{1.22}$$

where $\langle x^2\rangle$ is the variance of the probability distribution.

Brownian Carnot Engine

The problem of physically isolating the particle from surrounding heat bath can be overcome by using the fact that for an adiabatic process(for classical systems) $\mathcal{P}v^\gamma = constant$ where $\mathcal{P}$ is pressure,v is volume and $\gamma = c_\mathcal{P}/c_v$ with $c_\mathcal{P}$ and c_v being the heat capacities at

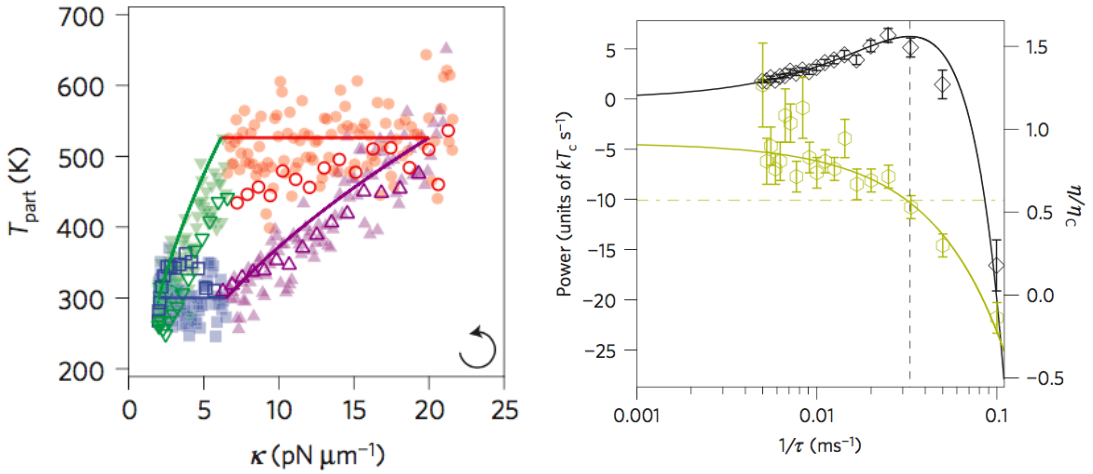

(a) (b)

Figure 1.7: (a) Temperature vs stiffness along a cycle: (1)isothermal compression(blue), (2)adiabatic compression(magenta), (3)isothermal expansion(red), (4)adiabatic expansion (b) Power (black diamonds), efficiency (yellow hexagons). This figure is adopted from [21].

constant pressure and volume respectively. In the framework of stochastic thermodynamics, for a spherical colloidal particle to undergo an adiabatic process, the Shanon entropy of the particle is constant. To maintain this condition, reservoir engineering and trap manipulation was simultaneously used by R.A. Rica and co-workers[21] . The environment temperature T and the trap stiffness k was manipulated in such a way that T^2/k was kept constant throughout the process.

By implementing these adiabatic transitions between the isothermal transitions of the the engine, Carnot cycles were realised and Curzon- Ahlborn curve for power was obtained for Brownian Carnot engines (Figure 1.7).

1.2.3 Active Mediums and Active engines

Apart from the artificial micro machines there are many microscopic biological machines present in nature [30, 36, 15]. One good example is a molecular motor. One key difference between these machines and the artificial heat engines is that these machines operate in a non-equilibrium active environments. This is due to the fact that in a complex environment like biological systems, there are plenty of driving forces rising from many chemical potential gradients. Thus the fluctuations in the properties of the micro machines are

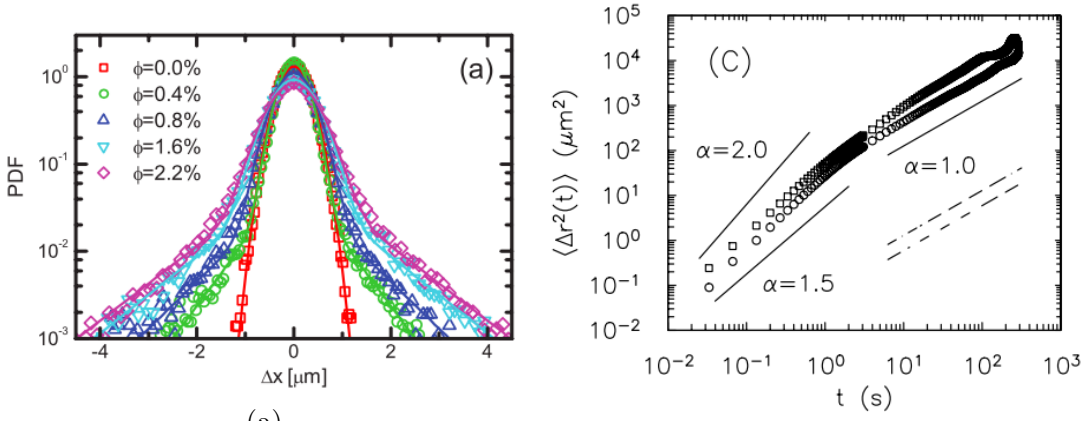

(a) (b)

Figure 1.8: (a) Probability distribution function of the tracer particle's displacement with respect to various concentrations of the active swimmers in the medium. This sub-figure is adopted from [19]. (b) mean squared displacement(msd) of the tracer particle in a suspension of active swimmers. This sub-figure is adopted from [37].

bound to deviate from a Gaussian. So to understand these machines better one should check the properties of simple artificial machines in environments with non-Gaussian fluctuations.

The simplest way to see non-Gaussian fluctuations in an artificial experimental system is to look at the tracer particle diffusion in a suspension of swimming eukaryotic cells or bacteria [37, 13, 19, 1, 10]. It has been seen that the PDF of the tracer particle's displacement [19] in such a situation has a huge tail deviating from Gaussianity and partly ballistic(super diffusive) and correlated motion [37] has been observed over time scales much larger than the time between the collisions from the solvent molecules(Figure: 1.8).

These sort of behaviours of the tracer particle trajectory has been identified due to the flows and jets created by the collective motion of the micro-organisms present in the medium. But if one thinks of the situation as an effective thermal bath then the exact nature of the fluctuating force is fairly unknown.

Active Heat Engine

The first attempt to understand the effect of activity as stated above on the performance of a Brownian heat engine was made by Krishnamurthy et al. [18]. In this experiment, Stirling cycles were performed on a trapped colloid in a medium containing bacteria as active swimmers. As expected the probability distribution function of the particle in the trap has heavy tails deviating far from a Gaussian (Figure 1.9). Although equipartition is not valid in this case, one can define an effective temperature T_{eff} from the width of the probability distribution function according to equation (1.22). From such kind of PDFs the fourth moment of the distribution i.e. the kurtosis can serve as a measure of activity of the effective bath. Now during the isochoric transitions, temperature of the water was physically changed. This caused the change in the activity of the bacteria resulting in a change of effective temperature (width of the PDF) and the kurtosis of the distribution. It was found that the work done of this engine was three orders of magnitude larger than the work done of a passive engine operated between the same temperatures effectively (Figure 1.9). Therefore it is evident that the non-Gaussian nature of the noise from an active environment has a huge effect on the performance of such micro machines.

The above engine was performed in the quasistatic limit. Whereas the the most practically relevant performance should be the one at maximum power. But it is impossible to study the Curzon Ahlbon curve of the power with this engine because of the fact that the bacteria take a certain amount of time to get activated and also remains active for a certain period even after the temperature is lowered. On the other hand It was found by Takahiro Sagawa and co-workers [16] that If two reservoirs with same noise intensity but with difference in the higher order moment of the noise is coupled, heat flow occurs between them.

At this moment two very important and fundamental questions can be asked about the operation of micro-machines in an active environment.
Firstly, if non-Gaussianity has this huge effect on the performance of a Brownian heat

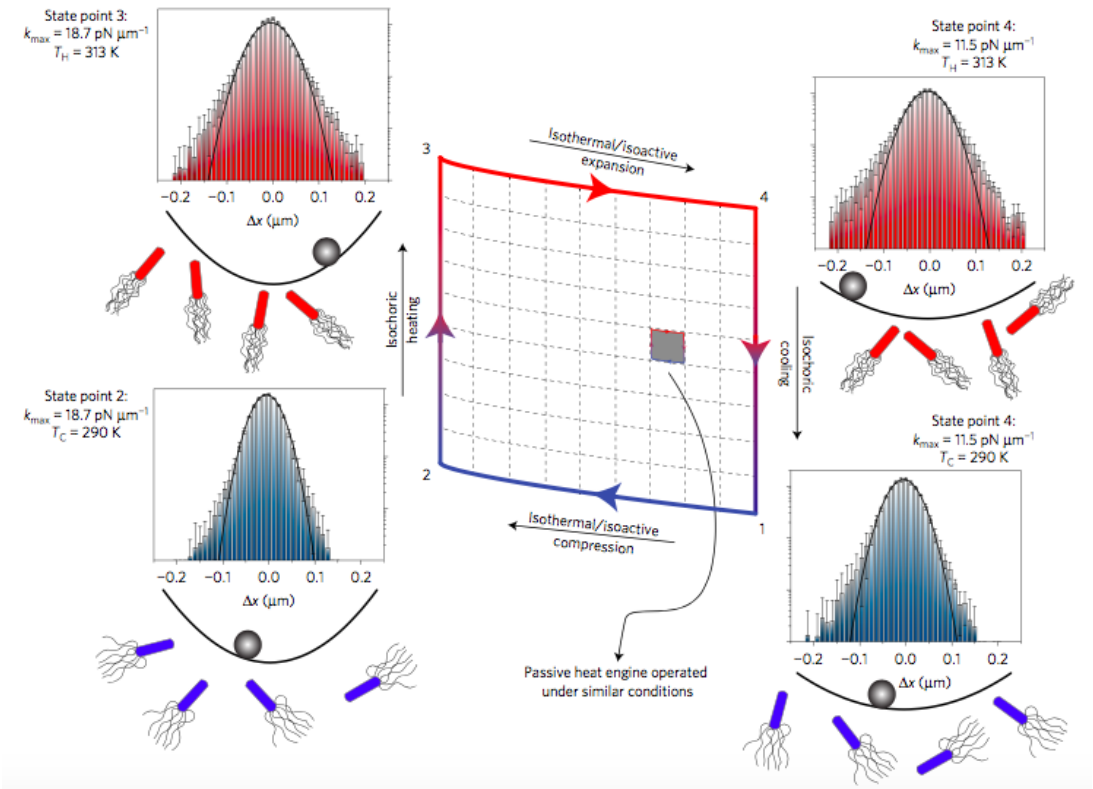

Figure 1.9: Schematic diagram of the operation of an active Stirling engine: Black curves are Gaussian fit to the histograms. Data points out side the Gaussian fit contributes largely to the kurtosis and thus to the work done. Area under the $\mathcal{P} - v$ diagram is the average work done per cycle with the grey shaded region corresponding to the work done for a passive engine operating between same temperatures and similar conditions. This figure is adopted from [18].

engine, is it possible for a Brownian engine to work only due to the difference between the non-Gaussianities of the two reservoirs? In other words, is it possible for an active Brownian engine to extract work in isothermal conditions?

Secondly, What will be the nature of the Curzon-Alhborn curve for such an engine?

In the next chapter the experimental methods to address these two questions will be discussed.

Chapter 2

Experimental Section

This chapter will discuss the experimental development made to design an active Brownian engine with engineered reservoirs. To experimentally realise an active Brownian engine operating in isothermal(in the sense of effective temperature) condition, the colloidal particle in the optical trap has to be alternatively coupled to two reservoirs which have the same noise intensity (i.e. variance of the PDF of particle's displacement being the same in the two reservoirs) but different kurtosis. As stated earlier, the enhanced kurtosis and the super diffusive nature of a tracer particle's motion in conventional active baths is due to the spontaneous and collective motion of the micro-swimmers in the medium which gives rise to flows and jets. So in this case, controlling and fine tuning the properties of the reservoir is extremely difficult. For example, one of the few trivial controls one can think of is changing the temperature of the medium physically. Now when the micro-swimmers are more active at a different temperature, both the noise intensity and the kurtosis of the PDF increases and the desired isochoric transitions becomes impossible.

Reservoir engineering turns out to be one tempting solution to this problem.

Electric field noise for a charged particle has been used so far to engineer a passive thermal bath [23]. To engineer an active reservoir, one needs to find out the nature of the noisy force acting on the tracer particle in an active bath. In the following section the

experimental setup capable of performing a Stirling cycle with engineered active reservoir has been described.

2.1 The Experimental Setup

2.1.1 The Cell

In the experiments, a Polystyrene sphere with a diameter of 5 micrometer (P[S/DVB] 5μm Bangslab) has been used as the working substance of the engine. The particle was suspended in a glycerol-water mixture(58%-42% by volume) inside a confined cell which is nearly 30 micrometers high. A very dilute suspension of the polystyrene beads is prepared so that there is only one particle in the field of view during the experiments. Two aluminium foil pieces (about 1mmX1mm in dimension) which are about 30 micron thick are used as a spacer to make the thin confinement cell. The solution is injected into the space between the cover slip and the slide with the help of capillary action. All sides of the cell is then sealed with UV curable glue (NOA 81). A schematic of the cell design is shown in Figure 2.1. This cell is kept on top of a 100x objective in the microscope (Leica DM13000B) and imaged with a fast camera (Photron 500K-M3) at 500 or 250 frames per second depending upon the duration of the experiment. Radial symmetry based tracking algorithm [25] was used to find the centre of the particle from the images.

2.1.2 Optical Arrangement

An alternative of noisy electric field can be through flickering optical traps in the vicinity of the colloidal particle. In this experimental setup we flash less intense(compared to the main trap holding the particle) optical traps at a frequency of 35Hz close to the particle.

To create this, we use two lasers, one to hold the particle in the solution and other to create small flickering traps around the particle. Now to create a system of several optical traps being dynamically reconfigured in space, several laser beams must be created falling at different angles on the back aperture of the microscope objective so that traps

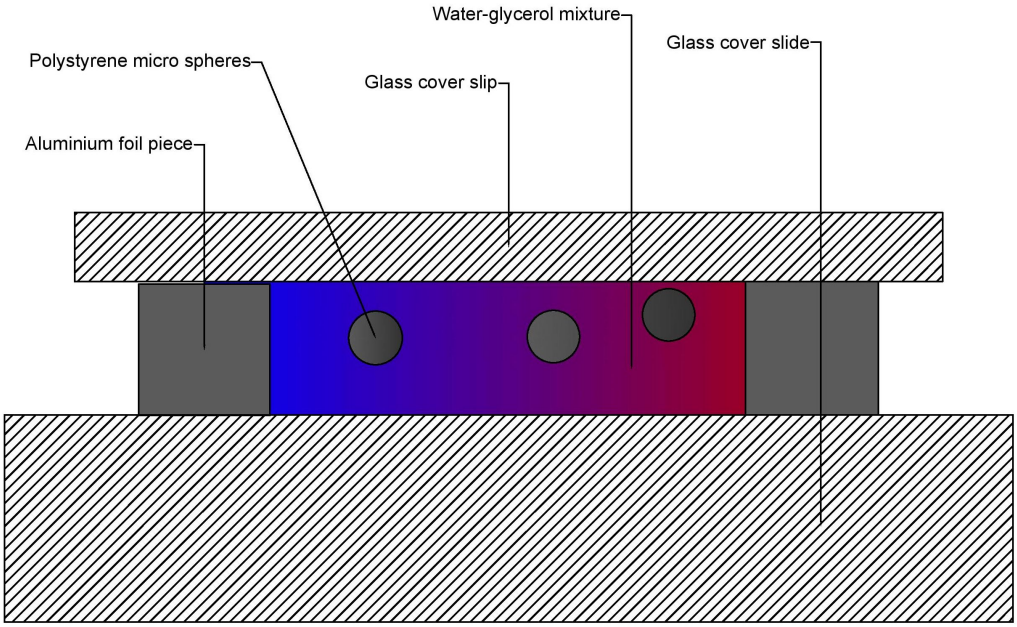

Figure 2.1: Schematic diagram of the confined cell used for most of the experiments.

get created at different positions after being focused by the microscope objective. This is achieved through Spatial light Modulator(SLM) [8, 6, 7, 11, 12, 24].

Spatial Light Modulator and Phase Modulation of the Secondary Laser

The SLM is a device which consists of a 2 dimensional array of tiny electrodes which can be given different electric potentials with computer control. On top of this electrode array there is a layer of liquid crystal. The molecules of the liquid crystal are rod shaped or elliptical and the orientation of these molecules can be manipulated by applying electric field. Now if different electric potentials are applied to different electrodes in the array, liquid crystal columns on each electrode attains different orientations as shown in Figure 2.2. The refractive index of a liquid crystal medium depends upon the orientations of its molecules. When a laser beam having a plane wavefront falls on the SLM (BNs XXX Phase) and gets reflected back by the shiny electrodes, different parts of the beam sees different refractive indices thus traverse different optical distances. Therefore by putting a configuration of electric potentials on the electrode, any desired phase pattern (pixelated)

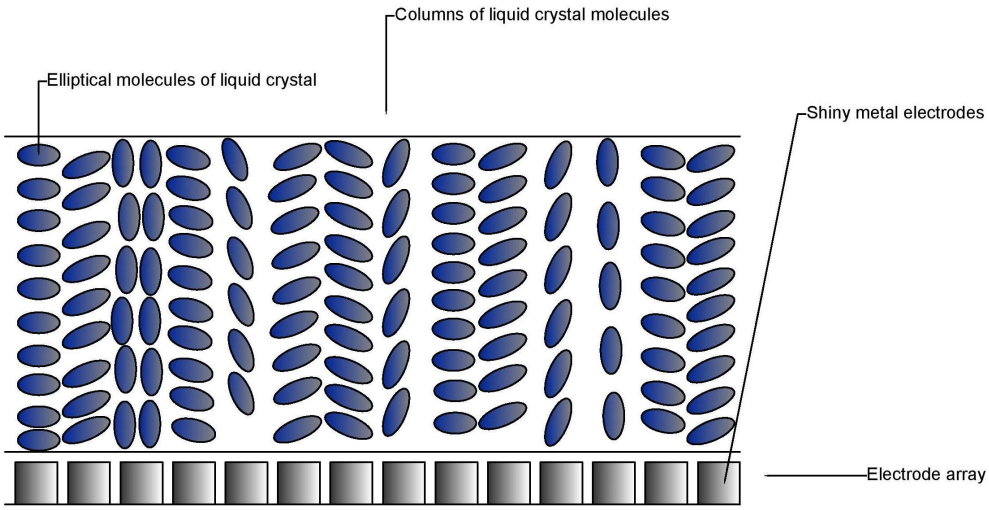

Figure 2.2: Schematic diagram of the Spatial Light Modulator with different electrode potential on the electrodes.

an be imposed on a laser beam. Now when the secondary wavelets of the laser beam coming out of the SLM propagate and interfere, a diffraction pattern forms which can be dynamically controlled by a computer (as shown in figure 2.3).

One of the simplest ways to create an optical trap at a distance from the trap created by focusing the central beam is to impose a grating pattern(Figure 2.4) on the wavefront of the laser beam through the SLM. Thus the distance at which the first order traps are created can be controlled by changing the periodicity of the grating pattern. Also multiple laser beams can be generated by creating grating patterns for each beam and summing the corresponding phases to get a resultant grating.

Our experiments require only one trap being generated at a time at different distances from the central trap which can be achieved by changing the periodicity of the SLM grating (Figure 2.4) in real time.

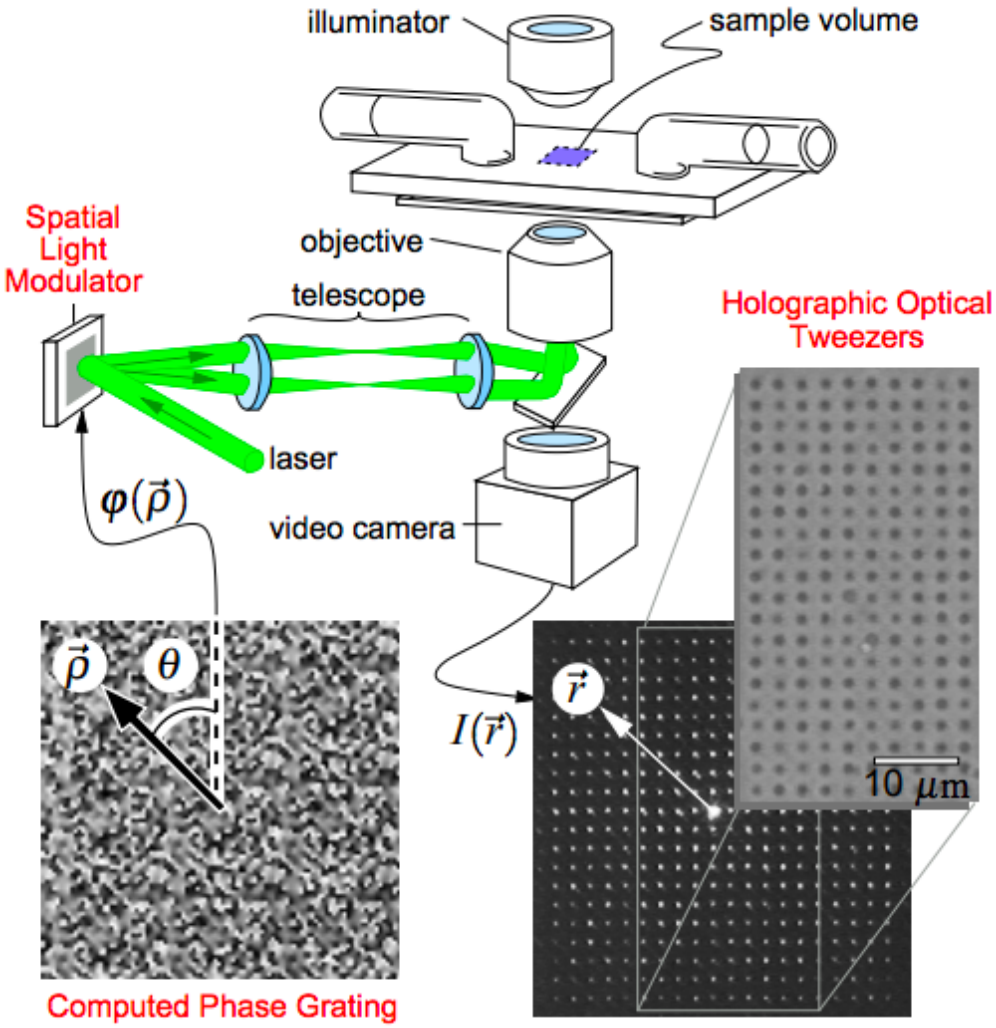

Figure 2.3: Schematic diagram to show how the phase pattern $\varphi(\rho, \theta)$ can create an array $I(\vec{r})$ after being focused by the microscope objective. This figure is adopted from [8]

Coupling Two Lasers to the Microscope

The primary trap holding the particle in the solution is created by focusing a 5W laser (ALS-IR-5-SF) by the microscope objective. This laser is operated at 0.5 W and the power is modulated by a motorized rotating half-waveplate before it enters the microscope objective. An 800 mW laser (Excelsior-PS-CDRH) is used to create the flashing traps which passes through the SLM.

A schematic diagram of the setup to couple both the lasers to the microscope is shown in Figure 2.5.

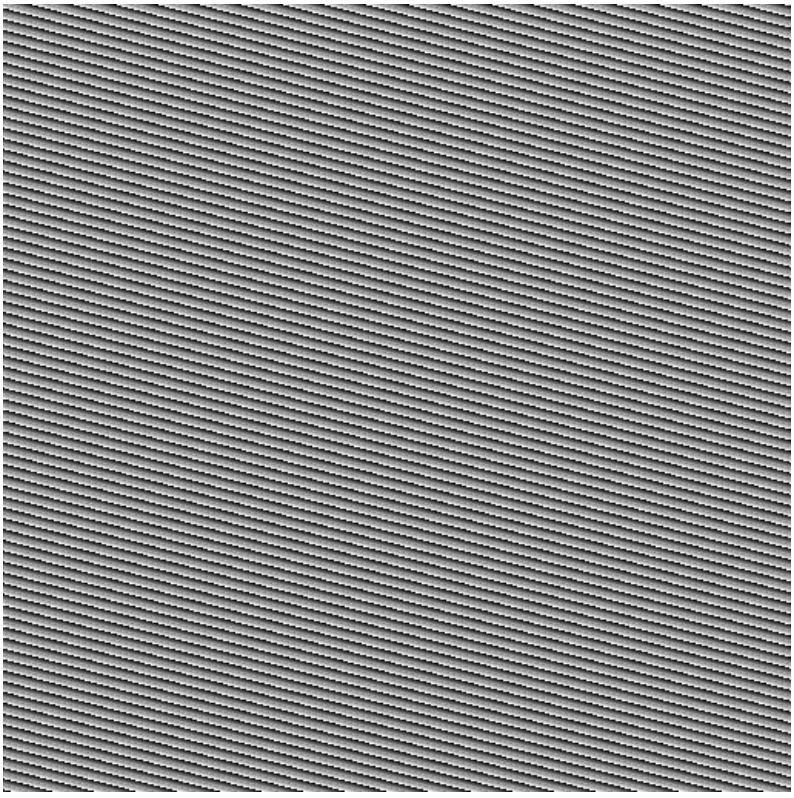

Figure 2.4: A sample grating pattern for the SLM used in our experiments.

The 5W laser (1064 nm) passes through a neutral density filter which cuts down its intensity by two orders of magnitude. The two lenses (one after the neutral density filter and the other before the microscope) in its path acts as beam expander and increases the beam diameter from 1.4 mm to roughly 6 mm which is the diameter of the back aperture of the microscope objective. The 50-50 beam splitter mirror allows 50% of the incident beam intensity to pass through it and reflects the other 50% towards the microscope. The beam splitter cube which transmits one component of the polarisation and reflects the other component, together with the rotating half wave-plate constitutes the power controlling circuit which varies the intensity and thus the trap stiffness linearly within a certain range which is maintained for all the experiments.

The power of the 800 mW (1064 nm) laser can also be controlled by manually adjusting the angle of the half wave-plate. The two lenses before the beam splitter cube in this optical path acts as the beam expanding circuit which increases the diameter of the laser beam from 0.4 mm to 6 mm. After reflection from the SLM a beam block is put on the

path of this laser in such a way that it blocks the central beam and allows the diffracted beams to pass through. The 50-50 beam splitter plate is adjusted in such a way that after reflection or refraction through the plate, both the 5W laser and the 800mW laser has the same optical path.

Finally all the lenses in the optical setup are adjusted in such a way that both the beams just before entering the microscope objective has the same divergence i.e. after being focused by the microscope objective, the optical trap created by both the lasers are roughly in the same plane which is perpendicular to the beams. The motorized half wave-plate and the SLM are connected to two computers which are again connected by an Ethernet cross-over cable so that rotating half wave-plate and the SLM can be operated in synchronization.

In the next section the exact protocols for realising engineered reservoir and Stirling

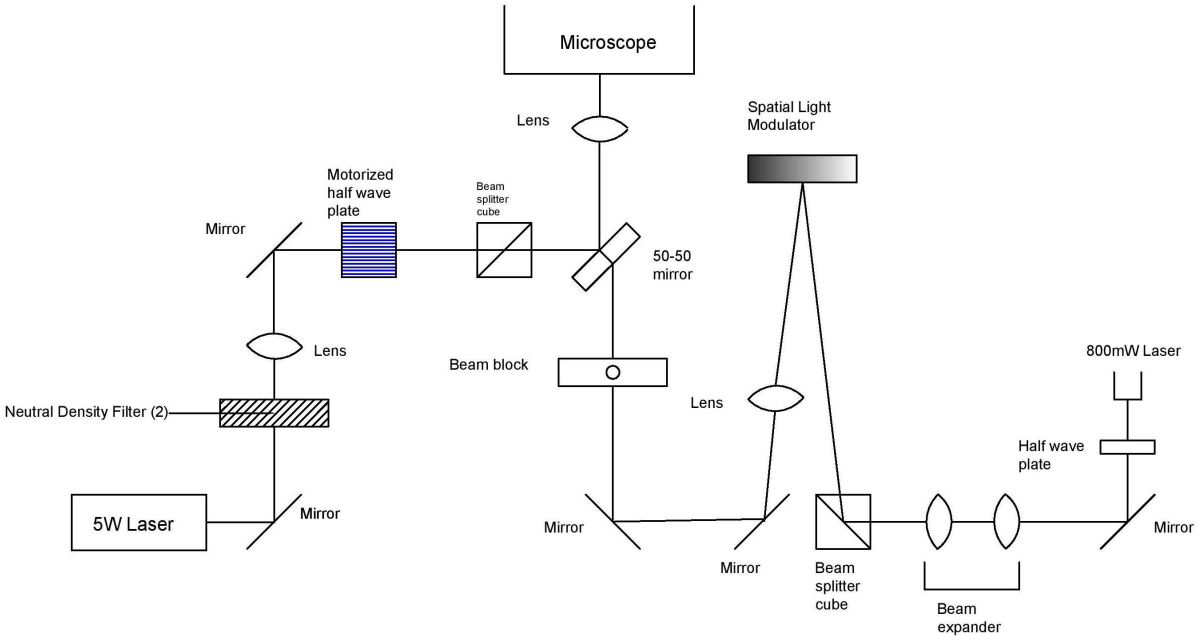

Figure 2.5: Schematic diagram for the arrangement to couple two lasers to the microscope

engine is discussed.

2.2 Experimental Protocols

Before moving on to active reservoirs and active Stirling engine, the validity of this specific technique for engineering reservoirs was checked by first engineering passive reservoirs and then reproducing the Curzon-Ahlborn curve for a passive Stirling engine operating between engineered thermal reservoirs with this technique.

2.2.1 Engineering Passive Reservoirs

In all the experiments, all quantities were measured in 1-dimension and the reservoir was engineered in one dimension as well. So to engineer the reservoirs, flickering traps are flashed along a straight line passing through the centre of the main optical trap holding the particle. The key idea of reservoir engineering with this technique is the fact that there is a one-to-one correspondence between the distance at which perturbing traps are flashed and the magnitude of the impulse that the particle feels due to these small flashing traps.
Therefore the external artificial noise is decided on the basis of the distances at which the small traps are flashed from the centre of the harmonic potential holding the particle. Now the thing to notice is that the particle in the harmonic potential is always being bombarded by the liquid molecules already and the position of the particle inside the trap is not fixed in the length scales at which the position of the particle is being measured and the perturbing traps are flashed.So the pre-decided noise being fed never works exactly as it should work for a static particle in the potential. As because the PDF of the particle's displacement from its mean position is a Gaussian with a mean zero, the noise works on the particle on an average as desired.

Let us consider the distance at which the perturbing traps are flashed from the centre of the harmonic potential to be $\delta x'$ in an arbitrary unit. To engineer passive reservoirs, $\delta x'$ is chosen from a Gaussian with a standard deviation σ'. The quantity σ' can be

meaningfully defined as the strength of the artificial noise.
It turns out that due to this kind of an artificial noise along with the noisy(Gaussian) force from the solution, the resultant PDF of particle's displacement is also a perfect Gaussian and one can determine the temperature of the effective engineered bath from the width of the resultant PDF as stated in equation 1.22. Figure 2.6 (a) shows how artificial noise with different strengths can be used to effectively increase or decrease the temperature of the particle (in an aqueous solution) much above and below the boiling or freezing point of water respectively with out physically heating or cooling the water. Figure 2.6 (b) shows that the corresponding power spectral density of the particle's vibration in the trap still remains Lorentzian which confirms that our artificial noise is acting as a Gaussian white noise on the overdamped particle.

It is also seen that the resultant temperature of the particle varies quadratically with the noise intensity as shown in figure 2.7. Therefore operating a Stirling cycle between a wide range of temperatures is possible.

2.2.2 Engineering Active Reservoirs

Although the exact nature of the noise on a tracer particle in a conventional active bath with complicated flows is unclear, some intuitive guess can be made from the properties of the PDF of the particle's displacement and also from the knowledge mean squared displacement of the particle with respect to time.

The PDF of particle's displacement in active baths, show a huge kurtosis deviating from a Gaussian. Now the huge enhancement of the 4th moment of the distribution i.e. kurtosis clearly indicates that there are always some drastic rare events happening with non-zero probability which causes very large displacements of the particle which are almost impossible in a thermal bath. Also the super-diffusivity at larger time scales indicate

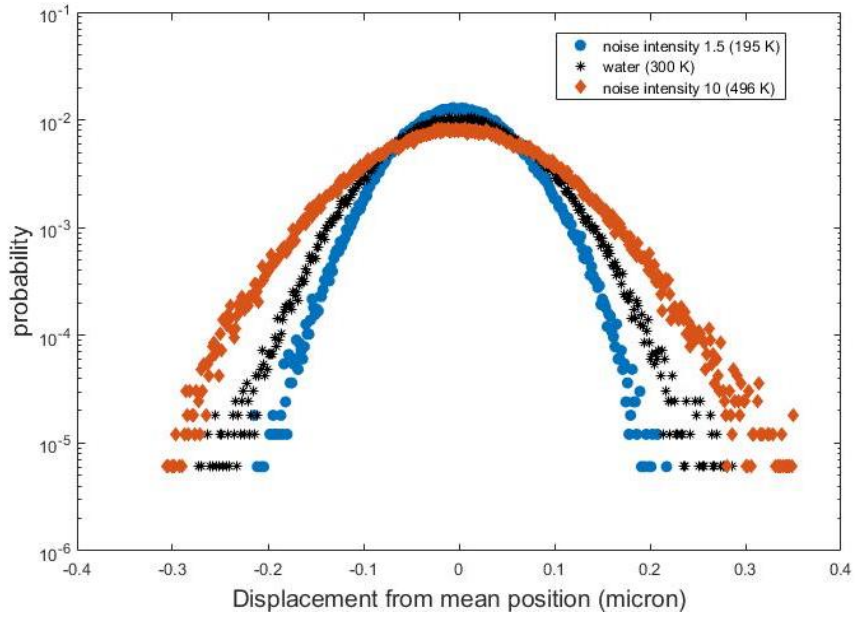

(a)

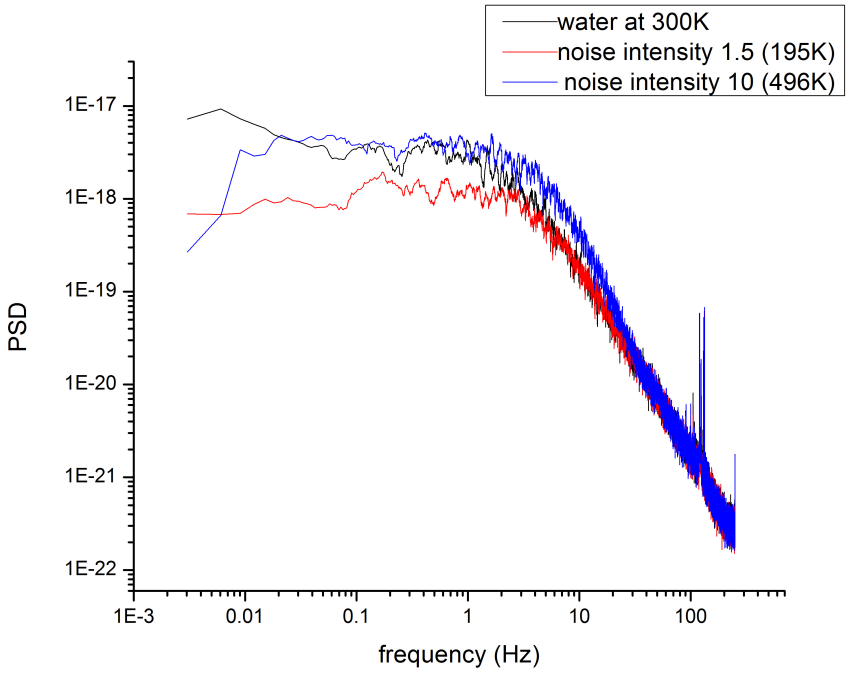

(b)

Figure 2.6: (a) PDF of particle's displacement with $\delta x' = 1.5$ (blue circles), without artificial noise (black stars) and with $\delta x' = 10$ (orange squares) corresponding to temperatures of 195K, 300K and 496K respectively. (b) Power spectral densities for the pre mentioned noise intensities.

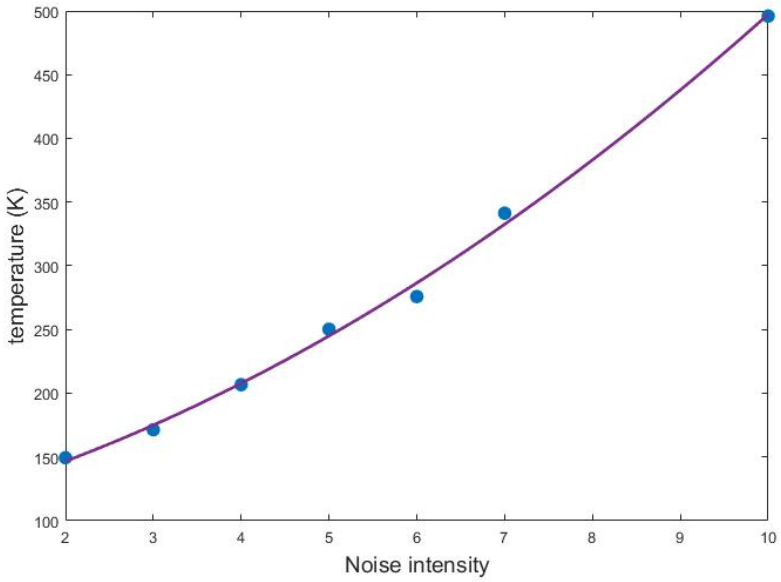

Figure 2.7: Blue circles are the temperature of the particle in the engineered reservoir with respect to the noise intensity, violet line is the quadratic fit.

that there are correlated motions which are impossible in a liquid in equilibrium.

So clearly the artificial noise for the engineered active reservoirs must cause the rare events when the particle's displacement is very high and thus it moves with a higher correlation. The distribution from which $\delta x'$s are chosen in this case, has a very high kurtosis close to 50 (shown in Figure 2.8 (a)). This distributions are created by taking the union and random permutation of the following two sets of random numbers generated by MatLab with function "$pearsrnd$".

Set 1: This set of random numbers has a skew of 6.5 and a kurtosis of 47 with a mean which is slightly shifted towards negative direction from origin.

Set 2: This set of random numbers has a skew of -6.5 and a kurtosis of 47 with a mean slightly shifted towards the positive direction from the origin.

In Figure 2.8 (a) the distribution is plotted against an index which runs from 1 to 22400 where the index 11200 corresponds to the position of the perturbing trap at the centre of the harmonic potential.

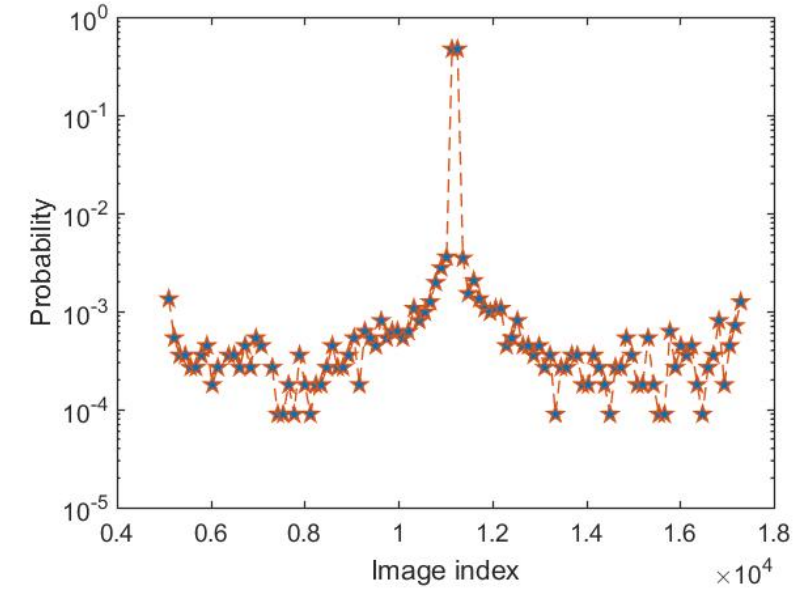

(a)

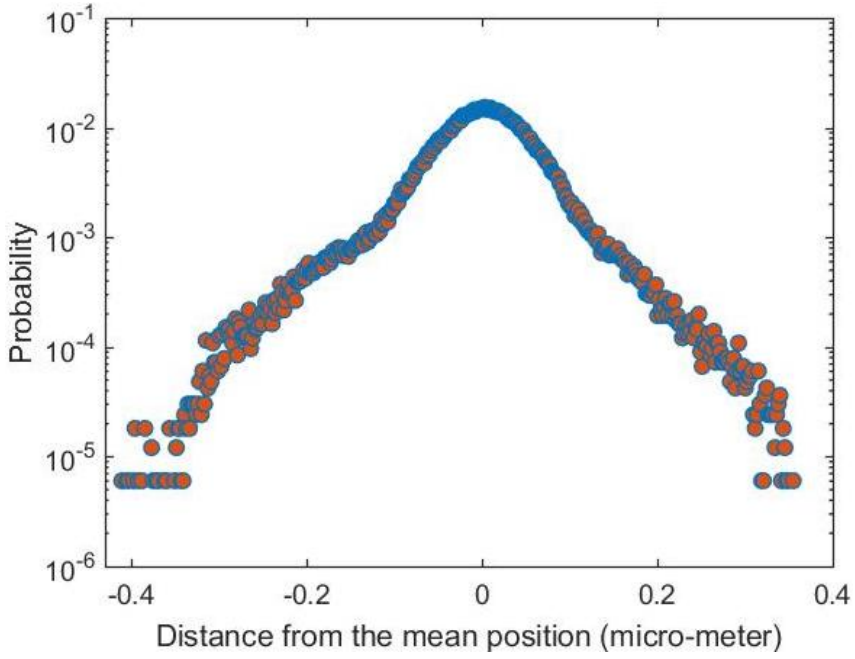

(b)

Figure 2.8: (a) Distribution of traps position with respect to an index running from 1 to 22400 where 11200th image(which are fed to the SLM) corresponds to the position of the perturbing trap at the centre of the harmonic potential (b) the resulting PDF of particle's displacement

The resulting PDF (Figure 2.8 (b)) of the particle's displacement form the mean has a huge kurtosis of 6 deviating far from a Gaussian (kurtosis=3) as it is expected to happen for a bath with active swimmers in it!

Once the heavy tailed PDF of particle's displacement has been created, it is trivial to implement it inside a Stirling cycle. So now with the aid of controlling temperature with the noise intensity, it is easy to create a thermal bath having the same width as the distribution in Figure 2.8 (b) with a kurtosis of 3. Thus it is possible to perform Stirling cycles between two reservoirs with the same noise intensity but only with different activity!

2.2.3 Protocol for the Stirling Cycle

The Stirling cycle starts out from the point when minimum trap stiffness k_{min} is maintained and phases corresponding to the lower isotherm is being flashed through the SLM. The series of operations involved to realise the Stirling cycle are as follows.

Step 1: The SLM starts flashing the phases corresponding to the lower isotherm and at the same time half wave-plate starts moving from angular position corresponding to k_{min} to the angular position corresponding to k_{max}.

Step 2: The motorized half wave-plate reaches the angular position corresponding to k_{max} after time $\tau/2$ and stops rotating further. As soon as the half wave-plate stops rotating, the SLM stops flashing the phases corresponding to lower isotherm.

Step 3: Just at the next moment the SLM starts flashing the phases corresponding to the higher isotherm causing an ideal isochoric transition and the half wave plate starts moving towards the k_{min} position.

Step 4: As soon as the half wave-plate reaches the k_{min} position and stops after a total time of τ from the initial state, the SLM stops flashing phases for the higher isotherm and starts flashing the phases for the lower isotherm causing another ideal isochoric transition.

Now depending upon the set of phases one chooses, realising Stirling cycle between any active or passive reservoirs is possible.

Chapter 3

Results and Discussions

In this chapter we discuss in detail the properties of the engineered reservoirs and quantify the performance of a stochastic Stirling engine operated between them and also shed a light on some of the fundamental aspects of the operation of micro-mechanical machines in different environments.

Reservoir engineering is emerging as a great tool to explore different aspects of the dynamics of systems at very small length scales and also as a powerful technique to optimise the operation of micro-machines in real world situations. As discussed in the previous chapter, putting external perturbations by flashing light fields around a dielectric particle turns out to be one of the elegant techniques to engineer reservoirs because of the following two reasons:

1. The magnitude of perturbing force is directly proportional to the distance at which the small traps are flashed from the centre of the harmonic potential. Because of the fact that this distance $\delta x'$ can be precisely controlled with SLM, force of any desired magnitude can be applied to the particle (see chapter 2).

2. With a maximum frequency of 33 Hz (limited by the SLM and the computer controlling it) time evolution of the force can be made in any arbitrary fashion.

The following section discusses how this method of reservoir engineering can effectively engineer thermal reservoirs and the properties of a Stirling engine operated between such

engineered reservoirs are exactly the same as those of an engine operated between real thermal reservoirs.

3.1 Stirling Engine Operated between Engineered Thermal Reservoirs

The most important physical advantage in using specifically this sort of engineered thermal reservoirs is that using this technique it is not only possible to effectively heat up the particle to very high temperatures, but also it is possible to effectively cool down the particle much lower than the temperature of the liquid or even lower than its freezing point which is not possible with other techniques of reservoir engineering. This ability of accessing a wide range of temperature makes it possible for some physical phenomenon to happen as discussed bellow.

3.1.1 Experimental Parameters

In our experiment the Stirling engine was operated between reservoirs with temperatures $T_c = 234\,Kelvin$ and $T_h = 260\,Kelvin$ corresponding to noise intensity σ' of 7.3 and 8.7 respectively in the glycerol-water mixture. During the isothermal transitions the stiffness of the harmonic potential was varied linearly between k_{min} and k_{max} to be equal to $602\,fN\,\mu m^{-1}$ and $766\,fN\,\mu m^{-1}$ respectively. Keeping this temperature difference constant, Stirling cycles were performed with cycle duration τ of 31.9s (60 cycles), 15.9s (78 cycles), 8.2s (200 cycles), 5.7s (200 cycles), 4,4s (200 cycles) and 3.7s (200 cycles).

3.1.2 Analysis of the Experimental Data

Now as the reservoir has been engineered in 1-dimension, all the quantities of the engine is measured in 1-dimension. Therefore the harmonic potential V in this case is given by

$$V(x,k) = \frac{1}{2}kx^2 \tag{3.1}$$

where x is the position of the particle with respect to the centre of the harmonic potential along the straight line on which the perturbing traps are flashed. All the quantities are measured from the knowledge of $x(t)$ and $k(t)$ at every time step.

Work done W with respect to time is calculated according to equation (1.11) and (1.13) with trap stiffness k being the control parameter (λ). Considering the fact that the particle is overdamped in the time scale of data acquisition (250 or 500 frames per second), the total force on the particle at any instant must be given by its position in the potential. So equation for work done becomes

$$W(x,t) = \int_0^t \frac{\partial V(k,x)}{\partial k}\dot{k}\, dt' = \int_{k(0)}^{k(t)} \frac{\partial V(k,x)}{\partial k}\, dk \tag{3.2}$$

with

$$\frac{\partial V(k,x)}{\partial k} = F_k = \frac{1}{2}x^2\,. \tag{3.3}$$

The work done dW_t in the interval $(t, t+\Delta t)$ is calculated from the discrete set of data $\{x_t\}$ using Stratonovitch's convention as follows:

$$dW_t = F_k(x_t,t) \circ dk_t = \frac{F_k(x_t,t) + F_k(x_{t+\Delta t}, t+\Delta t)}{2}\left[k_{t+\Delta t} - k_t\right] \tag{3.4}$$

Heat dissipation on the other hand is calculated using equation (1.14) from the knowl-

edge of force and the velocity of the particle. Now it is to be noted that the instantaneous velocity of the particle can not be approximated from the experimental data because the rate at which velocity fluctuates is much higher than the frequency of data acquisition. But it turns out that the average velocity $\langle \dot{x} \rangle$ of the particle during Δt amount of time can still be used under the integral to calculate heat exchanged [3]. Therefore heat dissipated during the time interval $(t, t + \Delta t)$ is calculated as

$$dQ_t = - \mid \frac{\partial V(x,t)}{\partial x} \mid_{(x_t,t)} \langle \dot{x} \rangle_t \, \Delta t = -k_t x_t \, \frac{x_{t+\Delta t} - x_t}{\Delta t} \, \Delta t \, . \tag{3.5}$$

So the work done W and heat Q as a function of time is calculated by taking the cumulative sum of the quantities expressed in equation (3.4) and (3.5). The work done per cycle and heat exchanges during the higher isotherm for every cycle with cycle duration τ is calculated from the knowledge of work done and heat as a function of time as follows:

$$W_{cycle} = W(t + \tau) - W(t) \tag{3.6}$$

and

$$Q_h = Q(t + \tau) - Q(t + \tau/2) \, . \tag{3.7}$$

Now with W_{cycle} and Q_h calculated, efficiency of the engine for the specific cycle is obtained as

$$\eta_\tau = \frac{W_{cycle}}{Q_h} \, . \tag{3.8}$$

3.1.3 Results and Discussions

The work done trajectory of the Stirling engine for maximum cycle duration of nearly 32s is shown in Figure 3.1(a). Here we see that this engine extracts out almost $1 k_B T_c$ of energy from the surroundings over 62 cycles of operation. From the zoomed in plot

in Figure 3.1(b) we see that during the first isothermal compression the work done is positive and thus the work is being done on the system while it is in contact with the cold reservoir. Then after the isochoric transition which does not show up in work done, $W(t)$ starts decreasing as a function of time during the isothermal expansion and the work is being done by the system. Now while in contact with the hot reservoir, work done by the system is on an average higher than the work done on the system during the isothermal compression. As a result the average work done per cycle is negative and the engine extracts out energy from its surrounding. Now according to stochastic thermodynamics the work done for a stochastic Stirling engine operated between the temperatures T_c and T_h and in the quasistatic limit is given by (similar to equation (1.20))

$$\overline{W}_{\infty} = k_B[T_c - T_h] \ln \sqrt{\frac{k_{max}}{k_{min}}}\,. \tag{3.9}$$

Putting the value of temperatures and the stiffness for our specific experiment, the theoretical value of $\overline{W}_{\infty}$ is $-0.0134 k_B T_c$. Using equation (3.6) the expectation value of efficiency for 32s cycle duration is found to be $\overline{W}_{32} = -0.0159\, k_B T_c$ which is in good agreement with the theoretical value. To further confirm that the engine is working in the quasistatic limit in $\tau = 32s$ cycle duration, we plot the distribution collapse of the PDF of the particle scaled with their corresponding stiffness throughout the higher isotherm as shown in figure 3.1 (c). In the distribution collapse the PDF of the particle is plotted against a scaled length x_k which is given by $x_k(k) = x * \sqrt{\frac{k}{k_{max}}}$. According to equation (1.22) if the PDF of the particle at different k values plotted against the variable x_k collapse on top of each other, the temperature of the particle is constant throughout the change of the traps stiffness which confirms the quasistatic reversible nature of the process. Again the efficiency of such an engine is theoretically given by

$$\eta_{\infty} = \frac{\eta_c}{1 + \frac{\eta_c}{ln(k_{max}/k_{min})}} \tag{3.10}$$

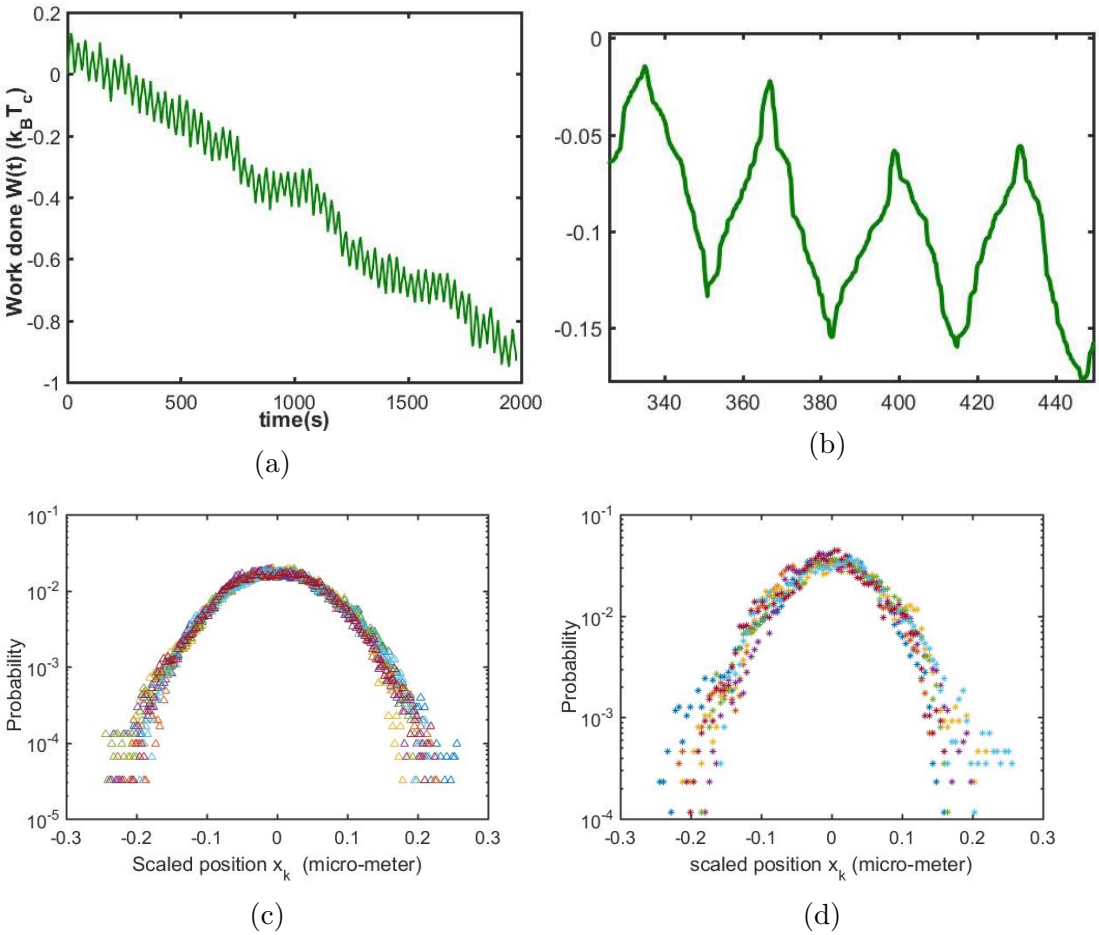

Figure 3.1: (a) Work done W as a function of time. (b) Zoomed in plot of the work done trajectory. (c)Distribution collapse of the particle's position scaled with trap stiffness x_k during the higher isotherm of the engine with $\tau = 32s$(d) Distribution collapse of the particle's scaled position x_k during the higher isotherm of the engine with $\tau = 4.5s$. It is very clear that the distributions do not collapse in this case.

where η_c is the Carnot efficiency and is given by

$$\eta_c = 1 - \frac{T_c}{T_h}\,. \tag{3.11}$$

For our experimental parameters, theoretical value of η_{inf} is 0.07. Using equation (3.8) the expectation value of efficiency for 32s cycle duration is 0.0829 which is pretty close to the theoretical value. Therefore at a cycle duration of 32s this engine operates in quasistatic limit as confirmed by the collapse of PDF of particle's position.

From the fluctuations in the work done trajectory as shown in figure 3.1 (b), it is

clearly seen that the work done per cycle is not constant for every cycle rather it is stochastic as expected for a system where the fluctuations have an important role in the dynamics. Now if one plots the probability density function of the work done per cycle, it turns out to be Gaussian as shown in figure 3.2 for cycle duration of 8.2s. This curve shows how the Gaussian nature of the noisy force on the particle ultimately shows up in the work done of the engine.

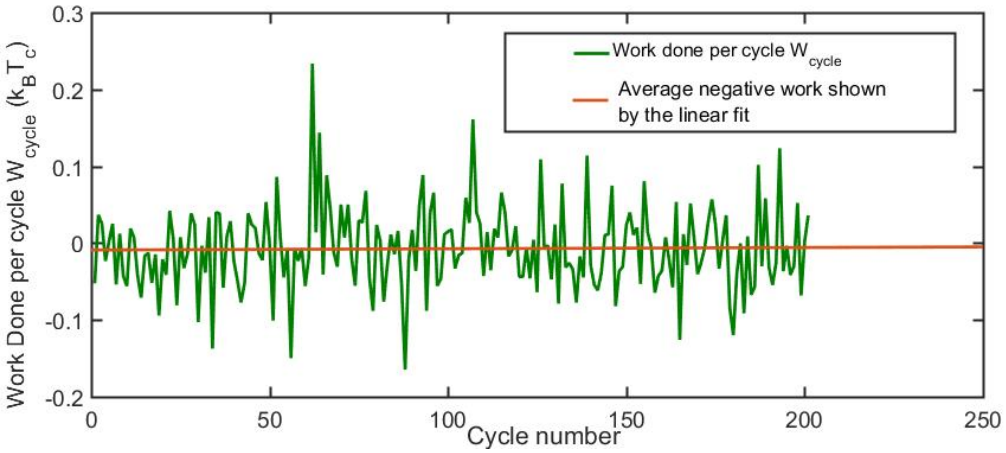

(a)

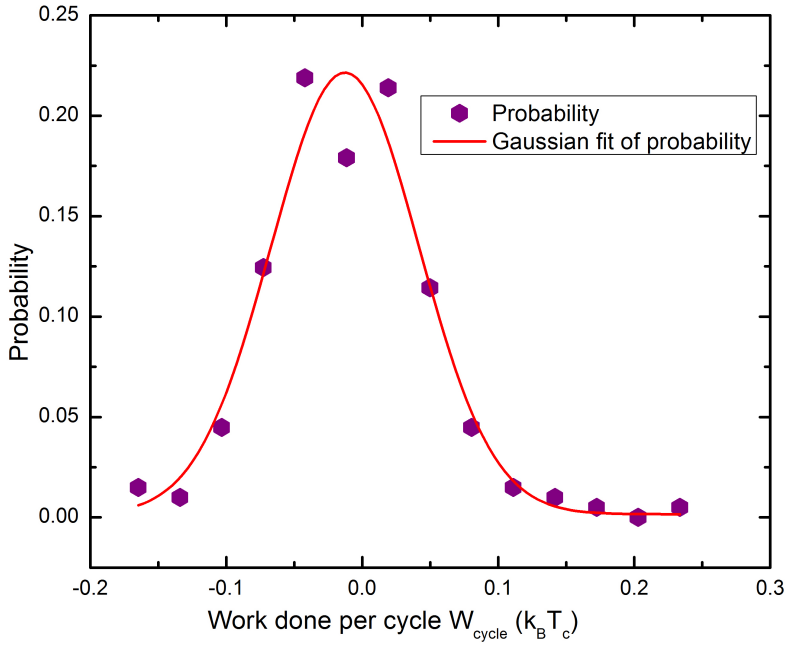

(b)

Figure 3.2: (a)Work done per cycle W_{cycle} with respect to cycle number. (b)Probability distribution function for work done per cycle for cycle duration $\tau = 8.2s$

Now as the cycle duration decreases the rate of change of trap stiffness from k_{min} to k_{max} increases and the particle gets lesser time to explore the volume available to it and thus the extent of equilibration for each stiffness $k(t)$. This causes an irreversible dissipative work done as shown in equation (1.19). From our experiments also we find that this irreversible dissipative component of the work done is always positive. As a result the magnitude of the work done decreases with cycle duration and for the cycle durations lower than 4.5s, the engine is no longer able to extract energy from its surrounding and the average work done is positive. The plot for work done as a function of cycle duration is shown in figure 3.3. Fitting work done versus cycle duration to the right hand side of the equation (1.19), we find that the positive irreversibility factor Σ is equal to 0.097.This quantity Σ serves as a good measure of irreversibility as larger Σ implies faster decrease of work done. It is also to be noticed that for smaller cycle durations the fluctuations in the work done is larger. This is another signature of building irreversibility can serve as an alternative measure of irreversibility in the operation of micro-machines in thermal environments.

Dividing both sides of equation (1.19) one finds the expression for power P of the engine as a function of cycle duration τ as following:

$$\overline{P} = \frac{\overline{W}_{\infty}}{\tau} + \frac{\Sigma}{\tau^2} \tag{3.12}$$

According to equation (3.12) the power P must have a maximum as suggested by Curzon and Ahlborn for macroscopic engines. Figure 3.4 shows how the power P of our Stirling engine between engineered reservoirs going through a maximum when plotted against cycle duration τ. Therefore the Stirling engine operated between these sort of engineered thermal reservoirs act exactly the same way as the ones operating between physical thermal reservoirs.

It was observed that when the same Stirling engine with same experimental parameters was operated between two engineered reservoirs at temperatures close to room tempera-

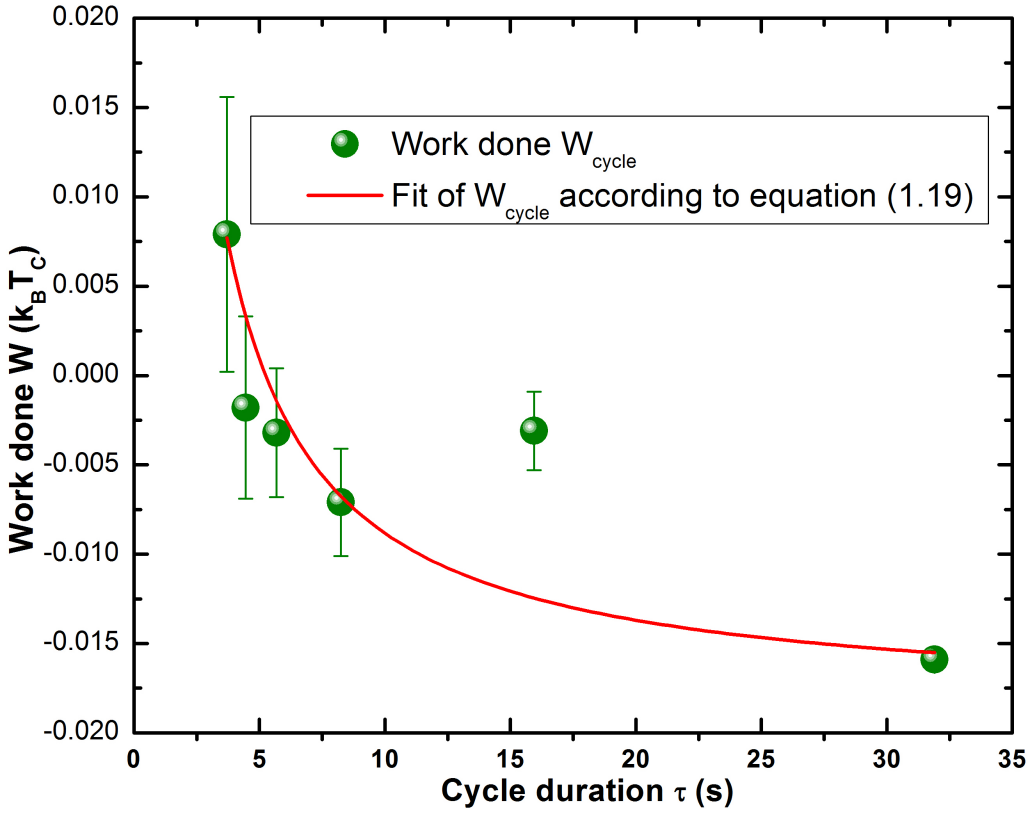

Figure 3.3: Work done per cycle W_{cycle} as a function of cycle duration τ

ture or higher, even at the lowest cycle duration of 3.7s neither stalling nor the maximum in the power was found rather the nature of work done or power was monotonic. This can be explained keeping in mind the fact that the nature of the work done or power curve with respect to the cycle duration is influenced highly by irreversibility. When at higher temperature, it is easier for the particle to equilibrate to a new trap stiffness because of the fact that at higher temperatures the range of the magnitude of the perturbing force is large and it is easier for the particle to span the volume available to it. Therefore probing irreversibility requires faster change of the control parameter $k(t)$ when the particle is at higher temperature. Thus one of the biggest advantages of this technique of reservoir engineering is that choosing the desired operating temperature range, any micro-mechanical machine can be operated in different modes such as maximum power or maximum efficiency without changing the experimental setup.

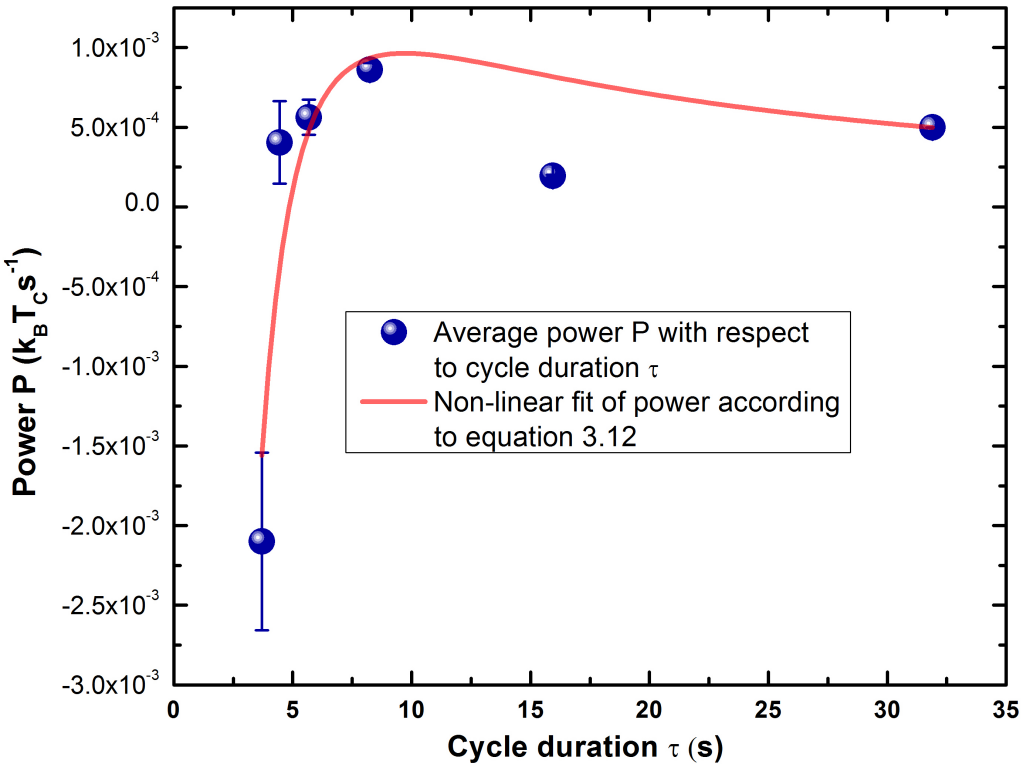

Figure 3.4: Power P of the engine with respect to cycle duration τ. This curve was predicted first by Curzon and Ahlborn for macroscopic heat engines.

3.2 Active Stirling Engine in Isothermal Conditions

As discussed in the previous chapter this method of reservoir engineering is able to engineer active reservoirs where the PDF of the particle's position has a huge kurtosis deviating far from a Gaussian. Furthermore, it is possible to realise two reservoirs which gives rise to the same noise intensity but different kurtosis. In order to do so, one reservoir was created by thermal reservoir engineering with a noise intensity σ' of 7.3 corresponding to temperature 243.7 K and the other was created with the protocol for engineering active reservoirs and has a kurtosis of 5.98 and the effective temperature of 241.2 K. The PDF of the particle's displacement in the two reservoirs is shown in figure 3.5.

Now in the Stirling cycle protocol, the active reservoir with the effective temperature of 241.2 K was chosen as the hot bath and the thermal reservoir with temperature 243.7 K was chosen as the cold bath so that in the Stirling cycle, the higher isotherm corresponds

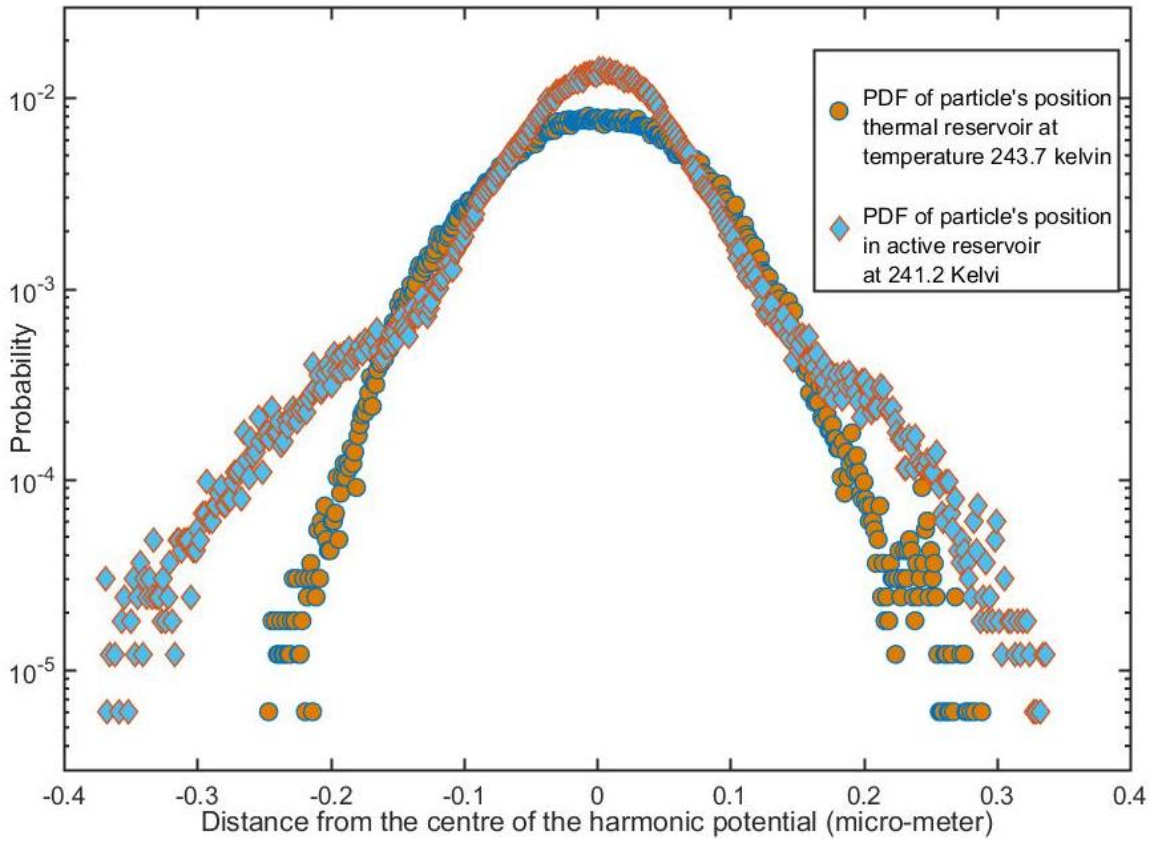

Figure 3.5: Diamonds: Heavy tailed (kurtosis = 5.98) PDF of the particle's displacement in the active reservoir. Circles: Gaussian PDF of the particle's displacement in thermal reservoir

to the isothermal expansion in contact with the active reservoir and the lower isotherm corresponds to the isothermal contraction in contact with the thermal reservoir. With the same potential as in the previous section, all the quantities were calculated in the same way as discussed in the previous section.

Now for this engine to perform work, the negative work done while in contact with the active reservoir has to be on an average higher than the work done on the system during the contact with the thermal reservoir. Figure 3.6 shows that the net work done for 31 cycles ($\tau = 32s$) of operation of this engine is negative. That implies even while operated between two reservoirs with same noise intensity, this engine is able to perform useful work.

This engine extracted $-0.178\, k_B T_c$ of energy from it's surroundings with an average

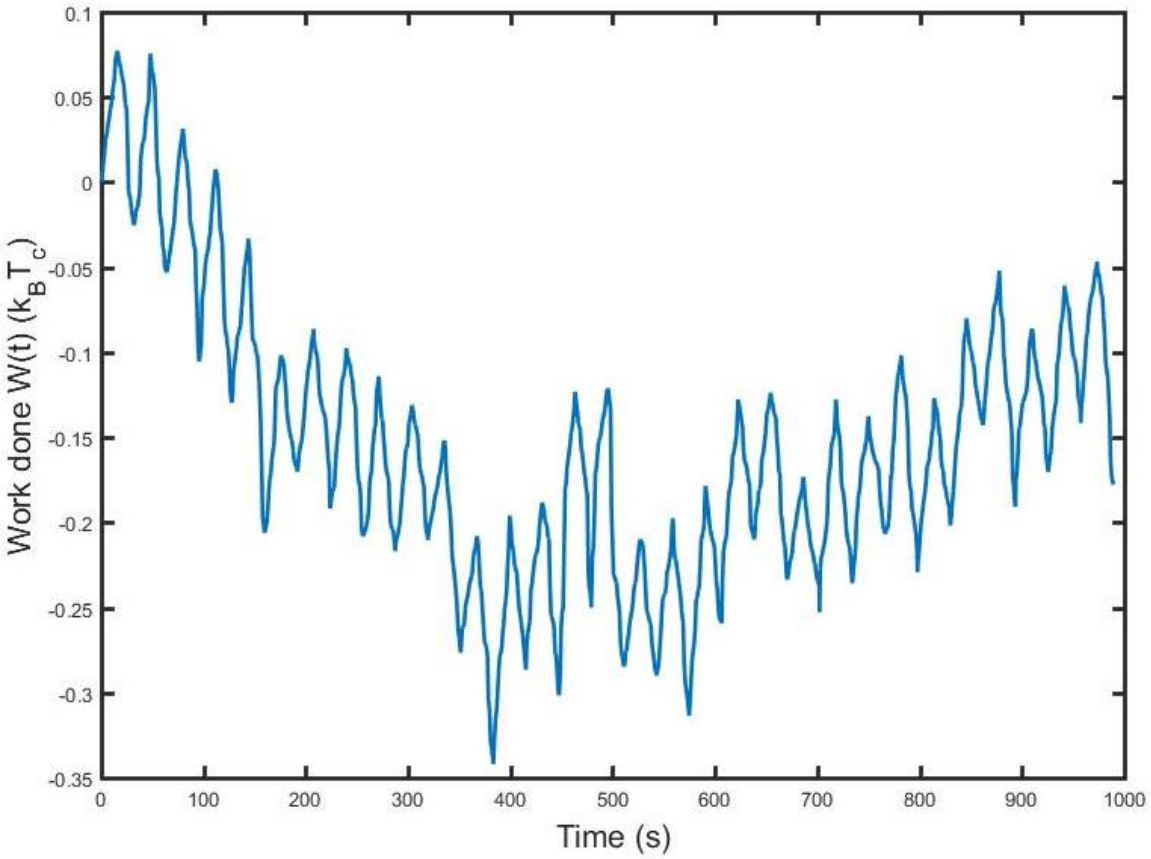

Figure 3.6: Work done trajectory of the Stirling engine operating between two reservoirs with the same noise intensity but difference in kurtosis.

work done per cycle $\overline{W}_{cycle}$ equal to $-0.0047\, k_B T_c$ with $T_c = 242\, Kelvin$. Only from the knowledge of noise intensity if one tries to find out the the quasistatic average work done and efficiency for this engine, they must turn out to be zero. Therefore the useful work done is mostly because of the rare events during the contact with the active reservoir which gives rise to very high displacements.

Although the histogram of the work done for this specific engine has not been checked due to lack of enough statistics, but from the work done trajectory it is very clear that the stochastic work done does not have a Gaussian fluctuation. The non-Gaussian nature of the fluctuations in the work done can be due to the fact that unlike the passive engine the nature of fluctuating force acting on the particle in this case is not Gaussian any more. This non-Gaussian nature of the fluctuation of the work done draws a deep connection

about how the work done out of a stochastic heat engine helps to interpret the nature of the environment.

3.2.1 Conclusions and Future Perspectives

In conclusion we can say that with this technique of reservoir engineering, not only it is possible to test the limitations of the performance of stochastic heat engines but also for the first time it has been made possible to realise an working Stirling engine operating between two reservoirs with the same noise intensity but different kurtosis. In future different cycle durations of such an isothermal engine between engineered active reservoirs will be studied to understand the role of irreversibility in non-equilibrium active dynamics and the performance of such heat engines.

The capability of such a novel technique of reservoir engineering is surely not bounded by mimicking reservoirs with active swimmers in it. Considering the versatility in the nature of noise it is capable of producing, performance of micro-machines can be tested in much more complex environments similar to biological systems. Apart from micro-machines, different kinds of noise can be used to test fluctuation theorems and can serve accessing new realms by violating some of the fundamental assumptions of stochastic thermodynamics.

Bibliography

[1] Luca Angelani, Roberto Di Leonardo, and Giancarlo Ruocco. Self-starting micromotors in a bacterial bath. *Physical review letters*, 102(4):048104, 2009.

[2] Valentin Blickle and Clemens Bechinger. Realization of a micrometre-sized stochastic heat engine. *Nature Physics*, 8(2):143, 2012.

[3] Valentin Blickle, Thomas Speck, Laurent Helden, Udo Seifert, and Clemens Bechinger. Thermodynamics of a colloidal particle in a time-dependent nonharmonic potential. *Physical review letters*, 96(7):070603, 2006.

[4] Jean-Philippe Brantut, Charles Grenier, Jakob Meineke, David Stadler, Sebastian Krinner, Corinna Kollath, Tilman Esslinger, and Antoine Georges. A thermoelectric heat engine with ultracold atoms. *Science*, page 1242308, 2013.

[5] Marie Chupeau, Benjamin Besga, David Guéry-Odelin, Emmanuel Trizac, Artyom Petrosyan, and Sergio Ciliberto. Thermal bath engineering for swift equilibration. *arXiv preprint arXiv:1801.09438*, 2018.

[6] Jennifer E Curtis and David G Grier. Modulated optical vortices. *Optics letters*, 28(11):872–874, 2003.

[7] Jennifer E Curtis and David G Grier. Structure of optical vortices. *Physical review letters*, 90(13):133901, 2003.

[8] Jennifer E Curtis, Brian A Koss, and David G Grier. Dynamic holographic optical tweezers. *Optics communications*, 207(1-6):169–175, 2002.

[9] FL Curzon and B Ahlborn. Efficiency of a carnot engine at maximum power output. *American Journal of Physics*, 43:22–24, 1975.

[10] R Di Leonardo, L Angelani, D Dell?Arciprete, Giancarlo Ruocco, V Iebba, S Schippa, MP Conte, F Mecarini, F De Angelis, and E Di Fabrizio. Bacterial ratchet motors. *Proceedings of the National Academy of Sciences*, 107(21):9541–9545, 2010.

[11] R Di Leonardo, J Leach, H Mushfique, JM Cooper, G Ruocco, and MJ Padgett. Multipoint holographic optical velocimetry in microfluidic systems. *Physical review letters*, 96(13):134502, 2006.

[12] Roberto Di Leonardo, Francesca Ianni, and Giancarlo Ruocco. Computer generation of optimal holograms for optical trap arrays. *Optics Express*, 15(4):1913–1922, 2007.

[13] Christopher Dombrowski, Luis Cisneros, Sunita Chatkaew, Raymond E Goldstein, and John O Kessler. Self-concentration and large-scale coherence in bacterial dynamics. *Physical review letters*, 93(9):098103, 2004.

[14] Shawn M Douglas, Ido Bachelet, and George M Church. A logic-gated nanorobot for targeted transport of molecular payloads. *Science*, 335(6070):831–834, 2012.

[15] Nobutaka Hirokawa, Yasuko Noda, Yosuke Tanaka, and Shinsuke Niwa. Kinesin superfamily motor proteins and intracellular transport. *Nature reviews Molecular cell biology*, 10(10):682, 2009.

[16] Kiyoshi Kanazawa, Takahiro Sagawa, and Hisao Hayakawa. Heat conduction induced by non-gaussian athermal fluctuations. *Physical Review E*, 87(5):052124, 2013.

[17] Jonne V Koski, Ville F Maisi, Jukka P Pekola, and Dmitri V Averin. Experimental realization of a szilard engine with a single electron. *Proceedings of the National Academy of Sciences*, 111(38):13786–13789, 2014.

[18] Sudeesh Krishnamurthy, Subho Ghosh, Dipankar Chatterji, Rajesh Ganapathy, and

AK Sood. A micrometre-sized heat engine operating between bacterial reservoirs. *Nature Physics*, 12(12):1134, 2016.

[19] Kyriacos C Leptos, Jeffrey S Guasto, Jerry P Gollub, Adriana I Pesci, and Raymond E Goldstein. Dynamics of enhanced tracer diffusion in suspensions of swimming eukaryotic microorganisms. *Physical Review Letters*, 103(19):198103, 2009.

[20] Ignacio A Martínez, Artyom Petrosyan, David Guéry-Odelin, Emmanuel Trizac, and Sergio Ciliberto. Engineered swift equilibration of a brownian particle. *Nature physics*, 12(9):843, 2016.

[21] Ignacio A Martínez, Édgar Roldán, Luis Dinis, Dmitri Petrov, Juan MR Parrondo, and Raúl A Rica. Brownian carnot engine. *Nature physics*, 12(1):67, 2016.

[22] Ignacio A Martínez, Édgar Roldán, Luis Dinis, Dmitri Petrov, and Raúl A Rica. Adiabatic processes realized with a trapped brownian particle. *Physical review letters*, 114(12):120601, 2015.

[23] Ignacio A Martínez, Édgar Roldán, Juan MR Parrondo, and Dmitri Petrov. Effective heating to several thousand kelvins of an optically trapped sphere in a liquid. *Physical Review E*, 87(3):032159, 2013.

[24] Miles Padgett and Roberto Di Leonardo. Holographic optical tweezers and their relevance to lab on chip devices. *Lab on a Chip*, 11(7):1196–1205, 2011.

[25] Raghuveer Parthasarathy. Rapid, accurate particle tracking by calculation of radial symmetry centers. *Nature methods*, 9(7):724, 2012.

[26] Muon Ray. Richard feynman "There's Plenty of Room at the Bottom". http://muonray.blogspot.in/2012/12/richard-feynman-theres-plenty-of-room.html, December 2012.

[27] Muon Ray. This is a lecture by Prof. Richard Feynman called "Tiny Machines". https://www.youtube.com/watch?v=4eRCygdW--c, August 2012.

[28] Johannes Roßnagel, Obinna Abah, Ferdinand Schmidt-Kaler, Kilian Singer, and Eric Lutz. Nanoscale heat engine beyond the carnot limit. *Physical review letters*, 112(3):030602, 2014.

[29] Johannes Roßnagel, Samuel T Dawkins, Karl N Tolazzi, Obinna Abah, Eric Lutz, Ferdinand Schmidt-Kaler, and Kilian Singer. A single-atom heat engine. *Science*, 352(6283):325–329, 2016.

[30] Manfred Schliwa and Günther Woehlke. Molecular motors. *Nature*, 422(6933):759, 2003.

[31] Tim Schmiedl and Udo Seifert. Efficiency at maximum power: An analytically solvable model for stochastic heat engines. *EPL (Europhysics Letters)*, 81(2):20003, 2007.

[32] Udo Seifert. Stochastic thermodynamics: principles and perspectives. *The European Physical Journal B*, 64(3-4):423–431, 2008.

[33] Udo Seifert. Stochastic thermodynamics, fluctuation theorems and molecular machines. *Reports on Progress in Physics*, 75(12):126001, 2012.

[34] Ken Sekimoto. Langevin equation and thermodynamics. *Progress of Theoretical Physics Supplement*, 130:17–27, 1998.

[35] Ken Sekimoto. *Stochastic energetics*, volume 799. Springer, 2010.

[36] Koen Visscher, Mark J Schnitzer, and Steven M Block. Single kinesin molecules studied with a molecular force clamp. *Nature*, 400(6740):184, 1999.

[37] Xiao-Lun Wu and Albert Libchaber. Particle diffusion in a quasi-two-dimensional bacterial bath. *Physical review letters*, 84(13):3017, 2000.